Gaseous mercury evasion from bare and grass-covered soils contaminated by mining and ore roasting (Isonzo River alluvial plain, Northeastern Italy)☆

Federico Floreani [a,b,*], Valeria Zappella [a], Jadran Faganeli [c], Stefano Covelli [a]

[a] Department of Mathematics and Geosciences, University of Trieste, Via E. Weiss 2, Trieste, Italy
[b] Department of Life Sciences, University of Trieste, Via L. Giorgieri 5, Trieste, Italy
[c] Marine Biology Station, National Institute of Biology, Fornace 41, Piran, Slovenia

ARTICLE INFO

Keywords:
Soil contamination
Hg mining
Gaseous Hg fluxes
Flux chamber
Vegetation
Cinnabar

ABSTRACT

High amounts of mercury (Hg) can be released into the atmosphere from soil surfaces of legacy contaminated areas as gaseous elemental mercury (Hg^0). The alluvial plain of the Isonzo River (NE Italy) suffered widespread Hg contamination due to the re-distribution of Hg-enriched material discharged by historical cinnabar mining at the Idrija mine (Slovenia), but an assessment of Hg^0 releases from the soils of this area is still lacking. In this work, Hg^0 fluxes at the soil-air interface were evaluated using a non-steady state flux chamber coupled with a real-time Hg^0 analyser at 6 sites within the Isonzo River plain. Measurements were performed in summer, autumn, and winter both on bare and grass-covered soil plots at regular time intervals during the diurnal period. Moreover, topsoils were analysed for organic matter content and Hg total concentration and speciation. Overall, Hg^0 fluxes tracked the incident UV radiation during the sampling periods with daily averages significantly higher in summer (62.4 ± 14.5–800.2 ± 178.8 ng m^{-2} h^{-1}) than autumn (15.2 ± 4.7–280.8 ± 75.6 ng m^{-2} h^{-1}) and winter (16.9 ± 7.9–187.8 ± 62.7 ng m^{-2} h^{-1}) due to higher irradiation and temperature, which favoured Hg reduction reactions. In summer and autumn significant correlations were observed between Hg^0 fluxes and soil Hg content (78–95% cinnabar), whereas this relationship was not observed in winter likely due to relatively low emissions found in morning measurements in all sites coupled with low temperatures. Finally, vegetation cover effectively reduced Hg^0 releases in summer (~9–68%) and autumn (~41–78%), whereas the difference between fluxes from vegetated and bare soils was not evident during winter dormancy due to scarce soil shading. These results suggest the opportunity of more extended spatial monitoring of Hg^0 fluxes particularly in the croplands covering most of the Isonzo River alluvial plain and where bare soils are frequently disturbed by agricultural practices and directly exposed to radiation.

1. Introduction

Mercury (Hg) is a widespread pollutant of global concern that poses serious threats to ecosystems and human health, mostly due to the neurotoxic effects of its methylated form (Boening, 2000; Clarkson and Magos, 2006). A peculiarity of this metal is the high volatility of its elemental form, often referred to as "gaseous elemental mercury" (hereafter Hg^0), which can be emitted to the atmosphere from both natural and anthropogenic sources (Pirrone et al., 2010). Once emitted, Hg^0 can persist in the atmosphere for more than 1 year (Saiz-Lopez et al., 2018) and thus be subject to long-range atmospheric transport before being removed through dry and wet depositions (Berg et al., 2008; Horowitz et al., 2017), even reaching remote areas (Kurz et al., 2019). Moreover, deposited Hg can be re-emitted back into the atmosphere from natural terrestrial and aquatic surfaces, thus the multiple surface-atmosphere exchanges can further expand its spread and residence time in the environment, a phenomenon previously referred to as "hopping effect" (Agnan et al., 2016; Jiskra et al., 2015; Lei et al., 2021).

Hg^0 exchanges at the soil-air interface represent a key aspect of the biogeochemical cycle of this element, with relevant Hg^0 emissions often reported for areas characterised by Hg-enriched substrates due to local geology and/or anthropogenic activities. These sites may constitute a

☆ This paper has been recommended for acceptance by Prof. Dr.Jörg Rinklebe.

* Corresponding author. Department of Mathematics and Geosciences University of Trieste Via E. Weiss 2, 34128, Trieste, Italy.
E-mail address: federico.floreani@phd.units.it (F. Floreani).

relevant secondary source of atmospheric Hg (Gustin et al., 2003; Kocman et al., 2013) where the magnitude of Hg^0 fluxes is primarily influenced by the total Hg (THg) concentrations in the substrate (Agnan et al., 2016). Generally, most Hg found in soil is present in oxidised forms (Hg^{2+}) (Anderson, 1979; Palmieri et al., 2006; Terzano et al., 2010; Beckers and Rinklebe, 2017) that must be reduced to the volatile form Hg^0 before being emitted (Carpi and Lindberg, 1998). The reduction of Hg^{2+} in soils can occur through abiotic pathways such as photoreduction, mostly mediated by UV radiation (Moore and Carpi, 2005), or reduction facilitated by interaction with functional groups of OM (Gabriel and Williamson, 2004) or iron-bearing minerals (Debure et al., 2020), but also Hg^{2+} reduction mediated by microbial activity can contribute to Hg^0 formation (Fritsche et al., 2008) as a detoxification pathway of mostly microorganisms containing the *mer* operon in their genome, activated by exposure to Hg (Mathema et al., 2011). On the other hand, Hg^0 adsorption on soil surfaces, favoured by its high affinity for reduced sulphur groups of organic matter (OM) as well as for iron and manganese minerals, can limit its vertical mobility through the soil (Schuster, 1991; Skyllberg and Drott, 2010; Yuan et al., 2019). As a result, Hg^0 volatilisation depends both on the rate of reduction reactions and on the sorption-desorption equilibrium between the soil matrix and pore space air (Carmona et al., 2013; Pannu et al., 2014), which in turn are influenced by several factors, e.g. incident solar radiation (Wang et al., 2005), soil and air temperature (Shi et al., 2020), precipitation and soil moisture (MacSween and Edwards, 2021), soil cover by vegetation and litter (Ma et al., 2018), soil disturbance (Sommar et al., 2016). These factors act in both contaminated and background areas (Miller et al., 2011), but their relative importance seems to be extremely site-specific (Agnan et al., 2016). Additionally, Hg speciation in soils deeply impacts its availability for reduction and subsequent volatilisation, as emissions are generally more rapid and intense where mobile and soluble forms of Hg are prevalent compared to sites dominated by insoluble forms such as cinnabar (α-HgS) (García-Sánchez et al., 2006; Kocman and Horvat, 2010; Llanos et al., 2011).

Anthropogenic inputs related to mining, coal combustion, and various industrial processes significantly affected the biogeochemical cycle of Hg and the amounts of the element circulating in the environment (Streets et al., 2019). The implementation of the Minamata Convention, aimed at phasing-out primary Hg mining and its use in precious metal extraction and industrial processes (Selin et al., 2018), is expected to reduce Hg emissions related to human activities. However, sites subject to past severe Hg pollution are able to emit high amounts of Hg^0 into the atmosphere even years after the primary source of contamination is no longer active, as evidenced by high Hg^0 fluxes recorded in areas contaminated by past mining (Dalziel and Tordon, 2014; Fantozzi et al., 2013; Kotnik et al., 2005) or industrial activities (Eckley et al., 2015; Osterwalder et al., 2019; Zhu et al., 2018). Understanding the fate of Hg in these areas is crucial to assess the potential exposure of the local population and wildlife to this metal and to evaluate possible mitigation and remediation strategies (Selin et al., 2018; Zhu et al., 2018).

The alluvial plain of the Isonzo River (NE Italy) is characterised by widespread Hg contamination as a consequence of historical Hg mining which took place at Idrija (Slovenia) from the 16th century until 1995 (Kotnik et al., 2005). Throughout ~500 years of exploitation, approximately 35,000 tons of Hg were lost in the surrounding environment (Dizdarevič, 2001) through atmospheric leaks and direct dumping of roasting residues on banks and riverbed sediments of the local Idrijca River, a tributary of the Isonzo River (Gosar et al., 1997; Žibret and Gosar, 2006), resulting in extended contamination of all environmental compartments (Bavec and Gosar, 2016 and references therein). Leaching and erosion of contaminated soils and sediments, mostly during rain events, favour the mobilization and transport of Hg to the Isonzo River and then finally to the northern Adriatic Sea (Baptista-Salazar et al., 2017; Pavoni et al., 2021). Due to flooding events, Hg has been re-distributed over the entire alluvial plain of the Isonzo River, resulting in high concentrations in soils (up to 76 mg kg^{-1}) which progressively decrease as the distance from the river increases (Acquavita et al., 2022; Cerovac et al., 2018; Piani et al., 2013). Few studies have highlighted the occurrence of Hg^0 atmospheric concentrations which are slightly higher than the natural background, mostly in the coastal sector of the southernmost part of the plain (Barago et al., 2020; Floreani et al., 2020), but a direct evaluation of potential Hg^0 releases at the soil-air interface is still lacking. The main aims of this study were to evaluate the Hg^0 emissions in selected sites along the plain characterised by a different degree of substrate contamination and to relate the results to soil Hg concentration and speciation and OM content in order to understand how differences in these parameters may influence the mobility of Hg at the soil-air interface. Hg^0 fluxes were measured in field by means of a manually operated non-steady state flux chamber coupled with a real-time portable Hg^0 analyser. This technique allows for a simple, rapid, and relatively cost-effective evaluation of Hg^0 evasion from the soil surface. Measurements were performed during the diurnal period in different seasons in order to verify the existence of any variability related to environmental parameters such as UV radiation and temperature. In addition, at each site Hg^0 emissions were measured over plots of bare and grass-covered soils in order to examine the potential influence of native vegetation cover.

2. Materials and methods

2.1. Study area

At the extreme eastern edge of the Friulian plain (Friuli Venezia Giulia Region, NE Italy), the Isonzo River alluvial plain is formed by quaternary sediments deposited during the Last Glacial Maximum by the Isonzo and Torre Rivers (Fontana et al., 2008) and is divided into two different geomorphological sectors (High and Low plain) by an East-West oriented Resurgence Belt (Cucchi et al., 2008; Treu et al., 2017). The southernmost coastal area of the plain adjacent to the mouth of the Isonzo River derives from hydraulic reclamation works carried out in past centuries to obtain cultivable areas from former lagoon and wetlands (Da Lio and Tosi, 2018; Marocco, 1989). Intense agriculture of prevalently maize and soybean occurs throughout the plain with the scarce presence of permanent meadows and a general increase in urbanisation and industrial settlements moving southwards (Acquavita et al., 2022; Contin et al., 2012; Salata et al., 2019). According to Rivas-Martínez et al. (2011), the bioclimate of the study area is classifiable as temperate oceanic, with relatively mild temperatures throughout the year and frequent precipitation. The annual mean rainfall in the area ranges between ~1000 and ~1400 mm moving from the coastal area to the High plain and the mean annual temperature is around 14 °C, with lowest values in January (~4.3 °C) and highest in July (~23.8 °C) (reference period: 1991–2021, data from ARPA FVG-Regional Agency for Environmental Protection of Friuli Venezia Giulia, through OSMER and GRN-Regional Meteorological Observatory and Natural Risk Management, respectively, https://www.meteo.fvg.it/). Local anemometry is determined by the breeze regime and synoptic winds from north-eastern direction, with episodic gusts of strong Bora winds (Giaiotti et al., 2003).

For this study, we focused on 6 sites along the plain (Fig. 1) near the present course of the Isonzo River located between 40 and 70 km downstream the confluence with the Idrijca River. The sites were selected on the basis of existing information about Hg concentrations in soils (Acquavita et al., 2022): 3 were located in the High plain, in the municipalities of Savogna d'Isonzo (SVI and SAV) and Sagrado (SAG), and the remaining in the Low plain near the villages of Turriaco (TUR), San Canzian d'Isonzo (SCZ) and Fossalon di Grado (FOS). The soils of the latter two sites are classifiable as Gleyic Fluvic Cambisols according to the World Reference Base for Soil Resources (WRB, https://www.isric.org/explore/wrb), whereas those of the other 4 sites belong to the group of Calcaric Fluvic Cambisols. Measurements of Hg^0 fluxes were

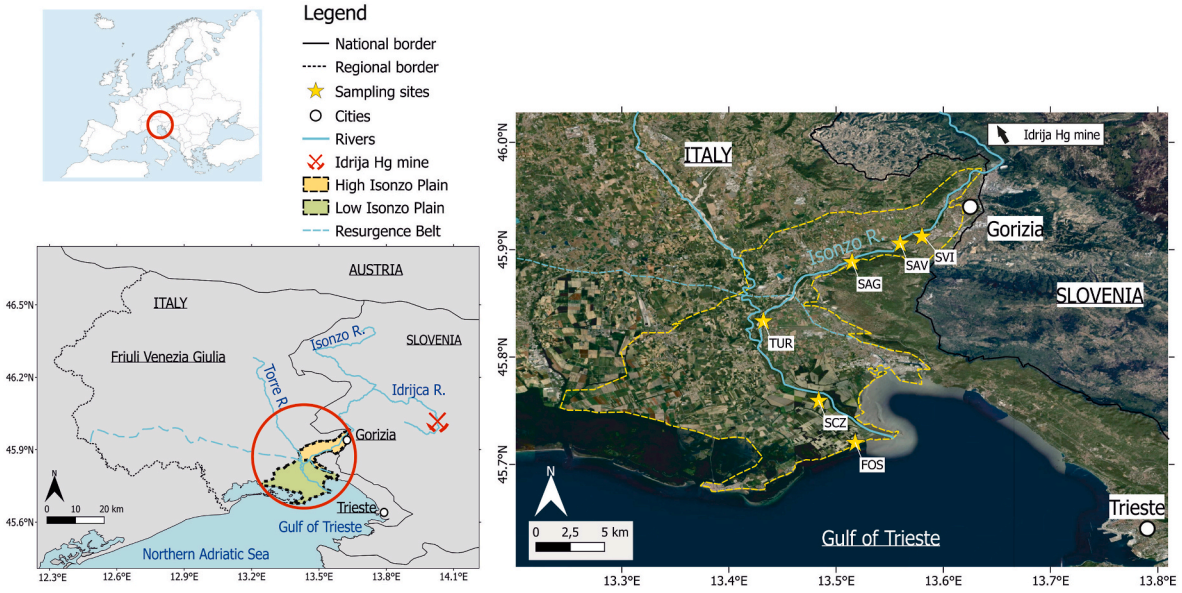

Fig. 1. Study area and location of sampling sites.

taken in meadows consisting of low lying non-woody vegetation. The sites referred to as SCZ and FOS were located near farmland soils with the occurrence of species such as *Setaria pumila*, *Cynodon dactylon*, *Artemisia vulgaris*, *Amaranthus retroflexus*. Conversely, sampling points at SVI, SAV, SAG, and TUR were located in permanent meadows along the course of the Isonzo River, which represent preserved natural environments with an important connectivity function in the ecological network in the context of regional landscape planning of the Friuli Venezia Giulia region (Sigura et al., 2017) and consequently protected as areas of relevant environmental interest (A.R.I.A.; Regional Law n. 42/1996). Common wild vegetation is dominated by *Poaceae*, including species as *Arrhenatherum elatius*, *Festuca arundinacea*, *Poa pratensis*, *Dactylis glomerata*.

2.2. Soil sampling and analysis

After Hg^0 flux measurements, topsoil samples (~0–2 cm) from each plot directly under the chamber were collected, sieved in the field at <2 cm to remove coarser particles, stored in clean polyethylene bags and taken to the laboratory, where an aliquot was immediately weighed for gravimetric determination of the moisture percentage. Plant residues of both aboveground (stems and leaves) and belowground biomass (roots) were carefully separated from the soil samples in the laboratory before analysis. Grain-size was determined only on samples collected in summer according to ISO 13320:2020 using a laser granulometer (Mastersizer 2000; Malvern Instruments Ltd., Worcestershire, UK). An aliquot (20 g) of fresh soil was used after a 24 h H_2O_2 (10%) treatment to reduce the bonding effect of the OM to the particles, followed by wet sieving at <2 mm and analytical determination on 2-mL aliquots.

For other determinations, a second aliquot of all soil samples was air-dried, gently disaggregated into a ceramic mortar, and sieved to 2 mm. Soil pH was measured with a glass electrode after equilibrating 5 g of soil with 12.5 mL of ultrapure water for 2 h according to Italian Decree 13/09/99. Organic matter content was determined as loss on ignition (LOI) at 550 °C (Heiri et al., 2001). Total Hg (THg) concentrations in soils were determined using a DMA-80 Direct Mercury Analyser (Milestone, Sorisole, Italy) atomic absorption spectrophotometer according to US-EPA Method 7374 (U.S. EPA, 1998). The limit of detection (LOD) was approximately 0.005 ng of Hg. A certified material (PACS-3 Marine Sediment Certified Reference Material, NRCC, Canada; Hg = 2.98 ± 0.36 mg kg^{-1}) was regularly analysed to verify the accuracy of the method and the obtained results showed acceptable recoveries (95–106%). The speciation of Hg in soil was evaluated following the thermo-desorption procedure described by Petranich et al. (2022). Briefly, approximately 80 mg of sample were progressively heated (0.5 °C s^{-1}) in a quartz boat from ambient temperature to ~700 °C in a furnace (Pyro-915+) coupled with a portable real-time gaseous Hg analyser (Lumex RA-915 M, Lumex Instruments, St. Petersburg, Russia) based on the atomic adsorption spectrophotometry technique with Zeeman background correction (Sholupov et al., 2004). A complete description of the thermoscanning unit was reported by Mashyanov et al. (2017). Temperature was continuously monitored through a type K thermocouple and the occurring Hg forms were identified by comparing their desorption temperatures with those of standard Hg compounds. The relative amounts of the different "thermospecies" were then determined by integrating the area under each desorption peak (Biester and Scholz, 1997) using the RAPID software (ver. 1.00.585) which controls the Lumex instrumentation.

2.3. Soil-air Hg^0 flux measurements

Hg^0 fluxes at the soil-air interface were evaluated during one diurnal period for each selected site in summer (July–September 2021), autumn (October–November 2021), and winter (January 2022). Hg^0 fluxes were not measured during spring, but considering that weather conditions and vegetation development in our study area in this season are not very much dissimilar to those encountered in autumn, it may be assumed that fluxes during these two periods are comparable. At each location, fluxes were measured in two adjacent sampling points, i.e. from soils characterised by the presence of native herbaceous vegetation cover and bare soil plots where grass was manually removed before sampling. Sampling points were chosen as close as possible to those previously used for the characterisation of Hg contamination of the Isonzo River plain (Acquavita et al., 2022). Flux measurements were performed by means of a Plexiglas non-steady state (NSS) flux chamber (60 × 20 × 25 cm) coupled with the Lumex analyser, which allows for the direct determination of Hg concentrations in the air in a wide dynamic range (2–30,000 ng m^{-3}). Operatively, the chamber was placed on the ground with edges inserted 1 cm into the soil fitting on a pre-installed stainless-steel frame. In order to achieve an optimal seal and minimise the intrusion of external air, soil was gently packed around the outer walls (Gillis and Miller, 2000). The Hg analyser was connected to the chamber in a closed

circuit through two Teflon tubes attached to 2 cm holes on the opposite short sides of the chamber. During the chamber deployment, air was recirculated through the system thanks to the Lumex internal pump at a constant flow rate of at least 10 L min^{-1}, creating a continuous gas movement over the soil surface (During et al., 2009). Due to the relatively high dimensions of the chamber, the use of a high air flow rate is required to provide a good level of mixing inside the chamber, necessary to obtain measurements of Hg^0 concentrations representative of the air in the chamber headspace (Maier et al., 2022). However, a high flow rate can potentially lead to bias in flux estimation due to pressure gradients between the outside and the inside of the chamber, particularly in highly permeable soils (Camarda et al., 2009; Davidson et al., 2002). To minimise the occurrence of pressure gradients between the outside and inside of the chamber and the disturbance on natural gas exchange processes at the soil-air interface related to the occurrence of advective fluxes between soil and air, two vents were placed on the upper wall of the chamber (Hutchinson and Livingston, 2001). However, these artefacts related to high flow rate are generally greater for open dynamic flux chambers (DFC) than for closed recirculation chambers due to the higher connection with ambient air (Camarda et al., 2009; Cotel et al., 2015). Concentrations of Hg^0 were continuously (every 1s) recorded for 5 min, as recommended for NSS chamber measurements using online real-time analysers (Maier et al., 2022), before removing the chamber. This short sampling time allowed for a reduction of the influence of the chamber on environmental parameters near the soil surface, such as temperature (Fantozzi et al., 2013; Rochette and Hutchinson, 2005), compared to DFC technique, more frequently adopted for Hg^0 soil emission measurement (Sommar et al., 2020). Thus, it was possible to take more distinct measurements from the selected points in a short time interval using the same Hg^0 analyser. Our chamber has a design similar to the DFCs used in other studies (e.g. Carpi and Lindberg, 1998; Sizmur et al., 2017) and coupled with a Lumex analyser (Fantozzi et al., 2013; García-Sánchez et al., 2006; Wang et al., 2006; Zhu et al., 2011) and our unpublished tests performed using both configurations (NSS and DFC) and the same air flow rate, comparable to those adopted in the cited studies, revealed a good agreement between fluxes measured with the two techniques ($r = 0.97$, $p < 0.001$, $n = 30$), with no systematic over- or underestimation of the flux calculated for the NSS technique compared to the well-established DFC configuration.

During each sampling day, Hg^0 fluxes were measured at regular time intervals of 1 h through 6/7 distinct set of measurements, each consisting of two consecutive replicate flux measurements conducted alternatively from bare and vegetated soil plots. The Hg^0 flux from soil (F) was then calculated from the increase of concentration inside the chamber during the enclosure (dC/dt) according to equation (1) (Bagnato et al., 2014; Kyllönen et al., 2012):

$$F = \frac{V}{A}\frac{dC}{dt} \quad (1)$$

where V is the internal volume of the chamber and A is the soil surface area covered by the chamber. As the increase of Hg^0 concentration inside the chamber can be assumed to be approximately linear for short chamber deployment times (Di Francesco et al., 1998; Kandel et al., 2016), the time derivative of Eq. (1) was quantified through the slope of Hg^0 concentration vs. time curve (Bagnato et al., 2014; Chiodini et al., 1998; Cotel et al., 2015; Davidson et al., 2002) and results were rejected if a good linear regression ($r^2 > 0.8$) could not be achieved (Kyllönen et al., 2012). Chamber blanks were determined daily by placing the chamber on a clean polycarbonate surface and the average value (1.6 ± 1.0 ng m^{-2} h^{-1}, $n = 18$) was subtracted to fluxes calculated from field measurements.

In parallel with soil-air Hg^0 fluxes, incident UV radiation between 250 and 400 nm were monitored in the field using a SU-420 sensor (Apogee Instruments, Logan, USA) mounted 2 m above ground near the sampling points. Data were logged every 1 min as the average value of readings taken every 1s. In addition, air temperature and relative humidity were measured using a portable thermohygrometer (HI9565, Hanna Instruments, Padova, Italy) which was also used to monitor the variation of these parameters inside the chamber headspace during the entire period of measurement (5 min) by inserting the probe in the chamber through a hole in the upper wall. Soil temperature was determined at a depth of 2 cm near sampling points using a thermal probe.

2.4. Statistical analyses

Statistical analyses were performed using R software ver. 4.1.3 (R Foundation, Vienna, Austria) and package *ggplot2* for data visualisation (Wickham et al., 2016). After checking data normality and homogeneity of variances with the Shapiro-Wilk and Bartlett tests, respectively, the statistical significance of differences between data groups was tested by means of Kruskal-Wallis (K–W) coupled with Dunn's post-hoc test. Pearson and Kendall correlation coefficients were used to assess the relationships between variables in the case of normal and non-normal data distribution.

3. Results and discussion

3.1. Physico-chemical characteristics of soils

General physico-chemical characteristics of investigated soils are summarised in Table 1. Overall, all the topsoils were characterised by a moderate alkaline pH (average = 8.09 ± 0.10), with no significant differences between samples collected at the same site in different seasons. In terms of grain size, silt was the predominant fraction at SAG (50.7 ± 0.9%) followed by sand (45.8 ± 1.1%) and clay (3.5 ± 0.2%), whereas the soils from all other sites showed a greater abundance of the sandy component (55.8 ± 4.5%) than the silty (40.9 ± 4.3%) and clayey (3.3 ± 0.9%) ones: according to United States Department of Agriculture (USDA) textural classification (USDA, 1987), these soils can be defined as *Sandy loam*, whereas samples from SAG fall in the class of *Silty loam* (Fig. S1).

The organic matter content was quite variable between sites, with the highest average value found at SCZ (17.51 ± 3.26%) and the lowest obtained for soils of FOS (2.92 ± 0.33%) in the reclaimed coastal area. The soils of the other sites were characterised by similar OM contents ranging on average between 8.30 ± 1.69% (SAG) and 10.76 ± 1.31%

Table 1
Overview of the main physico-chemical parameters of soil of the investigated study sites. Except for grain-size, data reported are the average (±std) values of all collected samples in the three different seasons.

	SVI	SAV	SAG	TUR	SCZ	FOS
pH	8.12 ± 0.06	8.17 ± 0.08	8.15 ± 0.08	8.14 ± 0.06	8.01 ± 0.05	7.96 ± 0.08
Sand (%)	53.8 ± 3.5	57.6 ± 6.2	45.8 ± 1.1	53.7 ± 2.8	55.0 ± 3.4	58.7 ± 5.4
Silt (%)	43.0 ± 3.0	40.0 ± 5.6	50.7 ± 0.9	43.6 ± 2.6	41.2 ± 2.7	36.9 ± 4.7
Clay (%)	3.1 ± 0.5	2.5 ± 0.6	3.5 ± 0.2	2.7 ± 0.2	3.8 ± 0.7	4.4 ± 0.8
LOI (%)	10.32 ± 1.00	10.76 ± 1.31	8.30 ± 1.69	8.93 ± 0.92	17.51 ± 3.26	2.92 ± 0.33
THg (mg kg^{-1})	16.58 ± 2.07	2.22 ± 0.50	17.22 ± 1.91	25.33 ± 4.12	8.01 ± 0.52	16.30 ± 3.66
α-HgS (%)	85 ± 2	94 ± 2	91 ± 2	94 ± 2	78 ± 1	90 ± 3
No-α-HgS (%)	15 ± 2	6 ± 2	9 ± 2	6 ± 2	22 ± 1	10 ± 3

(SAV), with little variability between samples collected in different seasons (Fig. S2+Table 1). Moreover, no significant differences were found between OM contents in topsoils from bare and vegetated plots for flux measurement.

3.2. Meteorological parameters

Field measurements for the determination of Hg^0 fluxes at the soil-air interface were performed under sunny weather conditions at almost all sites, except for sampling conducted at FOS in summer and autumn characterised by a more extended cloud cover and an irregular pattern of UV radiation during field operations. The highest UV irradiation was recorded during summer, with daily averages ranging from 29.7 (FOS) to 40.8 W m^{-2} (TUR), while minimum values were encountered in winter, when all single radiation measures were below 20 W m^{-2} (see Tables S1–S3). Air temperatures showed the same seasonal trend, ranging from 22.7 to 33.6 °C in summer, from 11.7 to 20.1 °C in autumn, and from −2.0 to 11.6 °C in winter with higher values typically recorded in the central part of the day and the minimum in the morning. Soil temperatures were similar and slightly higher than air in summer (27–34.5 °C) and on average colder in winter (−1.5-7 °C). In autumn relatively high values were recorded at TUR and SCZ, sampled in October (14–26 °C), whereas at other sites, sampled in November, soil temperatures were always below 15 °C (see Tables S1–S3). Generally, lower soil temperatures were found for vegetated than bare soil plots, particularly in summer due to the greater vegetation height and density which caused increased shading of vegetated soil and resulted in generally higher values of soil moisture (Fig. S3).

3.3. Total Hg concentration and Hg speciation in soils

The THg concentrations in the topsoils were quite variable. The average values considering all soil samples collected in the different seasons ranged from a minimum of 2.22 ± 0.50 mg kg^{-1} at SAV to a maximum of 25.33 ± 4.12 mg kg^{-1} at TUR. Intermediate and similar THg concentrations were found at SAG (17.21 ± 1.91 mg kg^{-1}), SVI (16.58 ± 2.07 mg kg^{-1}) and FOS (16.30 ± 3.66 mg kg^{-1}), whereas a slightly lower value was determined for SCZ (8.01 ± 0.52 mg kg^{-1}) (Table 1). These concentrations fall in the range previously reported for the entire area of the plain (<0.06–41.0 mg kg^{-1} from Acquavita et al., 2022), all exceeding the threshold level of 1 mg kg^{-1} established by Italian Decree 152/2006 for soils intended for public, private and residential use. Total Hg concentrations found in this study are one order of magnitude lower than those observed for soils of the Idrija Hg mining district (Bavec and Gosar, 2016; Teršič et al., 2011), undoubtedly due to the relevant distance from the source of contamination (Ottesen et al., 2013). However, no regular spatial pattern was found considering the selected sampling points along the Isonzo plain, suggesting that the observed concentrations could be dependent on irregular re-distribution of Hg-contaminated material by flooding events (Acquavita et al., 2022; Colica et al., 2019). In each site, no significant variations in terms of soil THg content were observed between bare and vegetated plots where Hg^0 flux measurements were performed (Fig. S4), and also the variability between samples collected from the same plot in different seasons was relatively limited and attributable to soil heterogeneity and to the uneven distribution of contaminated material even on a small spatial scale (Gilli et al., 2018; Rinklebe et al., 2009).

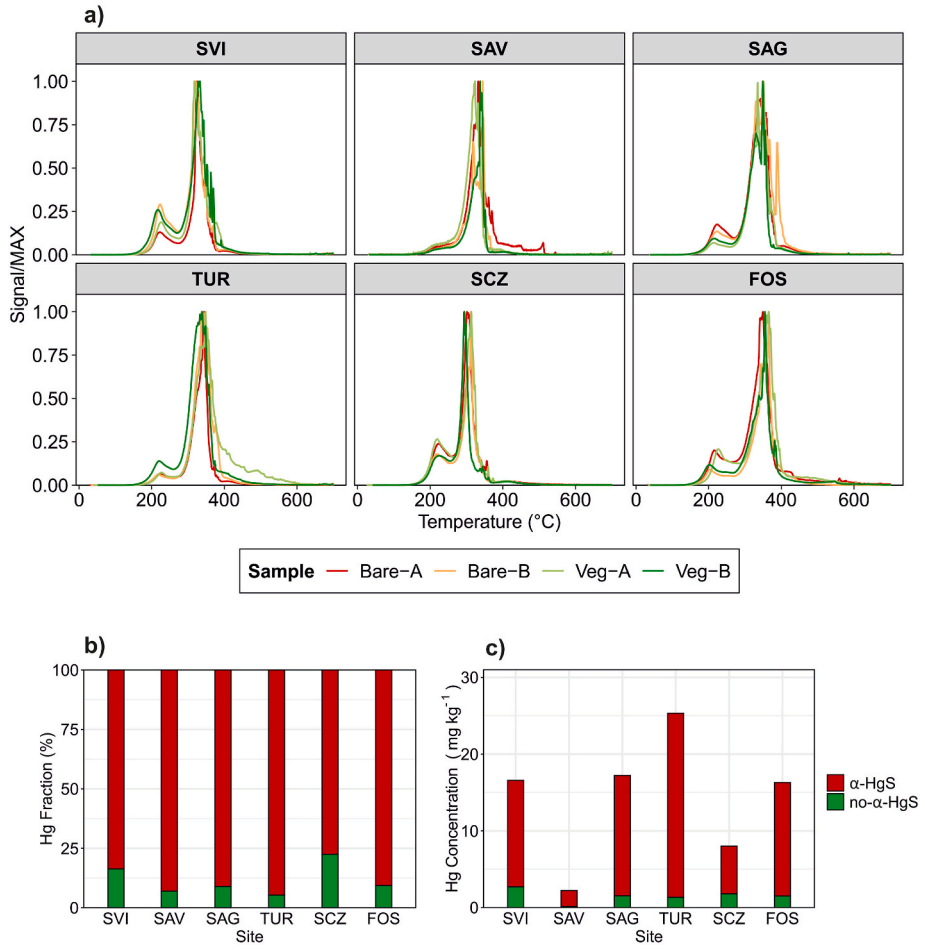

Fig. 2. a) termoscanning curves obtained from soil samples b) average percentage abundance of α-HgS and no-α-HgS fraction calculated from peak integration c) average concentrations of Hg extracted in the α-HgS and no-α-HgS fraction.

The thermal desorption profiles of all topsoil samples showed curves characterised by the presence of a double peak, with a first release between 200 °C and 230 °C and a second, more pronounced peak at temperatures ranging between ~300 °C and 365 °C (Fig. 2). According to the curves of standard materials reported by Petranich et al. (2022), the desorption temperature range of this second peak fits well with that of red cinnabar (α-HgS) from Idrija. This Hg form is considered the less mobile and bioavailable in soils (Gai et al., 2016; Pelcová et al., 2021) and its occurrence in our study area is likely the result of erosion and transport of α-HgS containing material from bottom sediments and riverbanks of the Idrijca River, where mining residues were directly discharged (Žibret and Gosar, 2006). Due to the incomplete decomposition during roasting process, these residues can still contain a certain amount of α-HgS (Esbrí et al., 2010; Yin et al., 2013). On the other hand, the first peak (200–230 °C) can be representative of the release of Hg from various non-cinnabar (no-α-HgS) forms which are potentially more mobile: similar desorption temperatures are indeed reported in the literature, e.g. for Hg bound to OM or to iron oxyhydroxides, and $HgCl_2$, but also for metacinnabar (β-HgS) (Biester et al., 2000; Coufalík et al., 2012; Petranich et al., 2022; Reis et al., 2015a; Rumayor et al., 2017). The occurrence of β-HgS as a by-product of ore roasting processes has been previously reported in mining residues discharged at Idrija (Biester et al., 2000; Teršič et al., 2011), whereas Hg bound to OM is present in notable amounts in the fine fraction of Idrija soils as a result of atmospheric depositions and is available for leaching and erosion during rain events (Baptista-Salazar et al., 2017). Based on the integration of peak areas, the contribution of this no-α-HgS fraction ranged from 5 to 22% of THg and is significantly correlated ($r = 0.67$, $p < 0.05$) to OM content, thus suggesting a contribution of the OM-bound Hg fraction, whereas Hg adsorption by iron oxyhydroxides can be considered less relevant in presence of relatively high concentrations of OM (Beckers and Rinklebe, 2017). The relative abundances of the α-HgS fraction (78–95%) are in good agreement with those of the non-mobile fraction determined by Acquavita et al. (2022) for the soils of the Isonzo River alluvial plain using a chemical sequential extraction procedure.

3.4. Hg^0 fluxes at the soil-air interface

Significantly ($p < 0.05$, K–W) higher Hg^0 fluxes were found for both bare and vegetated soils during the summer season compared to autumn and winter (Fig. 3). The greatest average fluxes for bare and vegetated soils were found at site TUR (800.2 ± 178.8 ng m^{-2} h^{-1}) and FOS (344.6 ± 36.2 ng m^{-2} h^{-1}) respectively, whereas the minimum values for both soil cover types in this season corresponded to site SAV (68.8 ± 21.6 and 62.4 ± 14.5 ng m^{-2} h^{-1}, respectively). This last site also provided the lowest average fluxes during autumn, respectively equal to 32.8 ± 10.1 and 15.2 ± 4.5 ng m^{-2} h^{-1} for bare and vegetated soils, whereas the highest values were found at FOS (280.9 ± 75.6 ng m^{-2} h^{-1} for bare soils and 102.6 ± 17.6 ng m^{-2} h^{-1} for vegetated soils). Finally, Hg^0 fluxes observed in winter varied from 187.8 ± 62.7 ng m^{-2} h^{-1} (FOS) to 40.0 ± 18.6 ng m^{-2} h^{-1} (SCZ) for bare soils and from 164.5 ± 36.1 ng m^{-2} h^{-1} (FOS) to 16.9 ± 7.9 ng m^{-2} h^{-1} (SAV) for vegetated soils. These values were the lowest of all the sampling campaigns for all bare soils with the exception of SAV, whereas they were slightly higher than the autumn averages from vegetated soils at SVI, SAV, SCZ, and FOS. However, differences between the average fluxes in autumn and winter were generally not significant ($p > 0.05$, K-M) except for emissions from bare soils at SVI, TUR and SCZ and from vegetated soil at FOS.

During some winter measurements, a peculiar trend for Hg^0 concentrations inside the chamber characterised by an abrupt change in the slope of the increasing curve after ~2 min of sampling was observed. This evidence concerned measurements taken in the morning hours over vegetated plots at SVI, SAV, TUR, and SCZ, when temperatures near or below 0 °C were observed coupled with a notable presence of frost on surfaces which can retain oxidised forms of Hg (Sherman et al., 2012), contributing to wet depositions (Converse et al., 2014). However, the majority of adsorbed Hg can be readily subject to photoreduction to Hg^0 and re-volatilisation (Ferrari et al., 2008), particularly when frost/ice is melting (Douglas and Blum, 2019). In our case, the chamber positioning may have caused a heating of the inside space due to high insolation, and a subsequent increase in frost melting and evaporation that may have led to the higher release of Hg^0 (Marsik et al., 2005), possibly influencing the build-up of the internal concentration. Consequently, for the calculation of Hg^0 emission from soil, only the first ~120 s after the initial period of ~20–30s (when the signal was affected by the disturbance caused by placing the chamber on the ground (Davidson et al., 2002)) were considered (Fig. S5).

The magnitude of Hg^0 releases observed in our study area impacted by the dispersion of Hg-enriched material derived from the Idrija Hg mine is in the range recently reported by Agnan et al. (2016) in a global database of Hg fluxes for mining sites, further confirming the importance of this activity in promoting high soil emissions. Moreover, values in the same order of magnitude of those presented in this study were previously reported for soils from Idrija (Kocman and Horvat, 2010; Kotnik et al., 2005) and for other sites impacted by various anthropogenic activities such as chlor-alkali plants, PVC production (Osterwalder et al., 2019; Zhu et al., 2018), metal smelters (Eckley et al., 2015), or coal combustion (Li et al., 2018). However, comparison with the literature should be interpreted with caution due to the different experimental setup adopted. Considering studies based on non-steady state systems, very low values have been reported for a boreal background forest in Finland (-1–3.5 ng m^{-2} h^{-1}, Kyllönen et al., 2012), whereas values similar to our study have been found for contaminated floodplains of the Elbe River in Germany (8.6–850 ng m^{-2} h^{-1}, Rinklebe et al., 2010; During et al., 2009). The NSS chamber approach is more frequently adopted in volcanic and geothermal areas using both

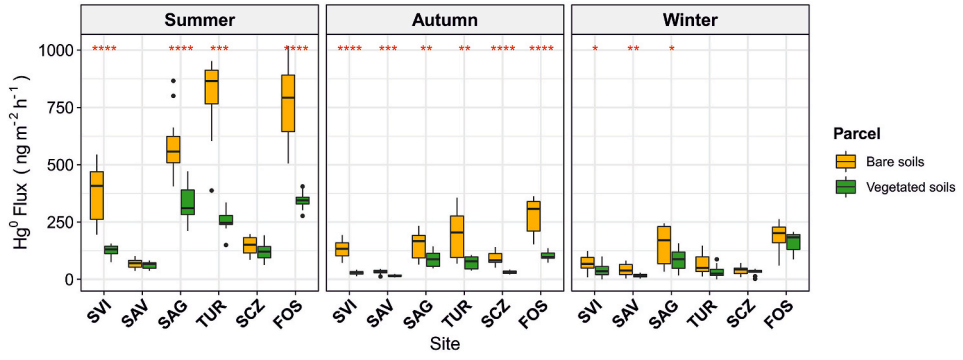

Fig. 3. Comparison among Hg^0 fluxes at soil-air interface from bare and vegetated soil plots in the various seasons; red asterisks indicate the statistically significant differences according to Kruskal-Wallis test (*$p < 0.05$; **$p < 0.01$; ***$p < 0.001$; ****$p < 0.0001$). (For interpretation of the references to colour in this figure legend, the reader is referred to the Web version of this article.)

dynamic systems with air recirculation inside the chamber (Bagnato et al., 2014; Sun et al., 2020a) and static systems without air movement in the inside space and periodic collection of gaseous samples for Hg^0 concentration analysis (Cabassi et al., 2021; Tassi et al., 2016). Regardless of the experimental setup adopted, Hg^0 emissions in these environments can reach values up to thousands or tens of thousands of ng m^{-2} h^{-1}.

3.4.1. *Effects of UV radiation and soil and air temperatures*

The above described seasonal variation of Hg^0 emissions from soils, with the highest values found during the warm season and the lowest in winter, has frequently been reported in various field studies (Eckley et al., 2015; Lei et al., 2021; Ma et al., 2018; Rinklebe et al., 2010; Shi et al., 2020; Wang et al., 2006). This seasonal pattern is usually related to temporal variations of parameters such as incident solar radiation and soil and air temperatures, which can synergistically regulate the release of Hg^0 at the soil-air interface (Ci et al., 2016; Ma et al., 2018). Solar radiation, particularly in the UV wavelength range, is effective in promoting the formation of Hg^0 through the photoreduction of Hg^{2+} in surface soils (Choi and Holsen, 2009a; Moore and Carpi, 2005), whereas high temperatures facilitate the desorption of bound Hg from organic and mineral surfaces due to increased vapour pressure and thermal motion (Carmona et al., 2013; Sigler and Lee, 2006) and lead to the expansion of gases, favouring the evaporation processes (Schlüter, 2000). Furthermore, increasing temperature can enhance reaction rates and microbial activity, resulting in a greater abiotic and biotic formation of Hg^0 (Pannu et al., 2014; Schlüter, 2000). Considering all the data collected in this study, Hg^0 fluxes from both bare and vegetated soils were significantly ($p < 0.001$) correlated with both average UV radiation calculated during the time of the single flux measurements and air and soil temperature measurements (Table 2), confirming the key role of these parameters in controlling the gaseous exchange of Hg at the soil-air interface (Beckers and Rinklebe, 2017). Negative relationships were generally found between Hg^0 fluxes and the relative humidity of the air (RH), likely due to the correlations existing between this variable and both incident radiation and air temperature, similar to that observed in other studies (Tao et al., 2017; Wang et al., 2006).

The relationship between Hg^0 fluxes and UV radiation was often stronger than those found between fluxes and both soil and air temperatures and may have been more relevant in controlling Hg^0 releases during our field measurements than thermal effects. This is consistent with results previously reported in other studies (Agnan et al., 2016; García-Sánchez et al., 2006; Liu et al., 2014; Wallschläger et al., 1999; Wang et al., 2005) and likely confirms that radiation, despite contributing to soil heating and subsequently to the thermal enhancement of Hg^0 fluxes, can also have an effect on Hg^0 evasion independent from that related to soil temperature (Bahlmann et al., 2006). Further research is needed to evaluate the possible contributions of Hg^0 formation and volatilisation related to biotic reduction mediated by Hg-resistant microorganisms, frequently isolated from Hg-contaminated soils (Mahbub et al., 2016) and also present in the Idrija Hg mine area (Bourdineaud et al., 2020; Campos-Guillén et al., 2014; Hines et al., 2000). The relatively scarce bioavailability of the α-HgS fraction predominant in our soils could have limited this contribution, but recent studies suggested that under particular conditions (i.e. after complexation) this form can also be taken up and transformed by microorganisms (O'Connor et al., 2019; Zhang et al., 2012).

The strong dependence of Hg^0 fluxes on UV radiation is also confirmed considering the variation of both parameters during the measurement periods over each individual day (Fig. 4 and Figs. S6–S10). Hg^0 fluxes generally increase in the morning up to a peak in the central part of the day and then decline in the afternoon, following the pattern of incident UV radiation, as already observed in several studies in various environments (Kyllönen et al., 2012; Shi et al., 2020; Zhu et al., 2018). The Hg^0 emission drop in the afternoon was particularly rapid at TUR (Fig. S9), where sampling points were shaded by surrounding trees. Conversely, soil temperatures showed a smaller fluctuation during the monitoring period, remaining almost constant during afternoon measurements in summer and showing slight decreases in autumn and winter. Moreover, during summer sampling at FOS the sun was intermittently hidden by clouds, resulting in an irregular variation of UV radiation and a corresponding trend of Hg^0 fluxes, whereas soil temperatures did not show notable variations (Fig. 4). These rapid changes of fluxes in response to changes in the UV radiation could reinforce the hypothesis that Hg^0 emissions at our study sites are more influenced by irradiation than soil temperatures (García-Sánchez et al., 2006; Zhu et al., 2011) and that the soil portion more involved in gaseous exchanges is restricted to a shallow surface layer more affected by incident radiation variations (Eckley et al., 2015; Sigler and Lee, 2006; Zhou et al., 2021). However, higher temperatures could explain the generally higher Hg^0 fluxes recorded in the afternoon than in the morning (excluding TUR) despite the comparable incident UV radiation levels.

Table 2
Kendall rank correlation coefficients (τ) among Hg^0 fluxes and environmental parameters values recorded in all seasons at the different sampling sites. The significance level is also reported (***$p < 0.001$; **$p < 0.01$; *$p < 0.05$).

	T soil (°C)	UV (W m^{-2})	T air (°C)	air RH (%)
Bare soils				
SVI	0.72***	0.75***	0.76***	-0.54***
SAV	0.43***	0.55***	0.46***	-0.32**
SAG	0.53***	0.74***	0.61***	-0.73***
TUR	0.80***	0.82***	0.78***	-0.34**
SCZ	0.69***	0.78***	0.76***	0.41***
FOS	0.76***	0.65***	0.79***	-0.10
Vegetated soil				
SVI	0.42***	0.69***	0.45***	-0.59***
SAV	0.53***	0.61***	0.60***	-0.16
SAG	0.51***	0.74***	0.57***	-0.65***
TUR	0.80***	0.78***	0.79***	-0.37**
SCZ	0.46***	0.60***	0.49***	0.32**
FOS	0.39***	0.62***	0.37***	-0.16

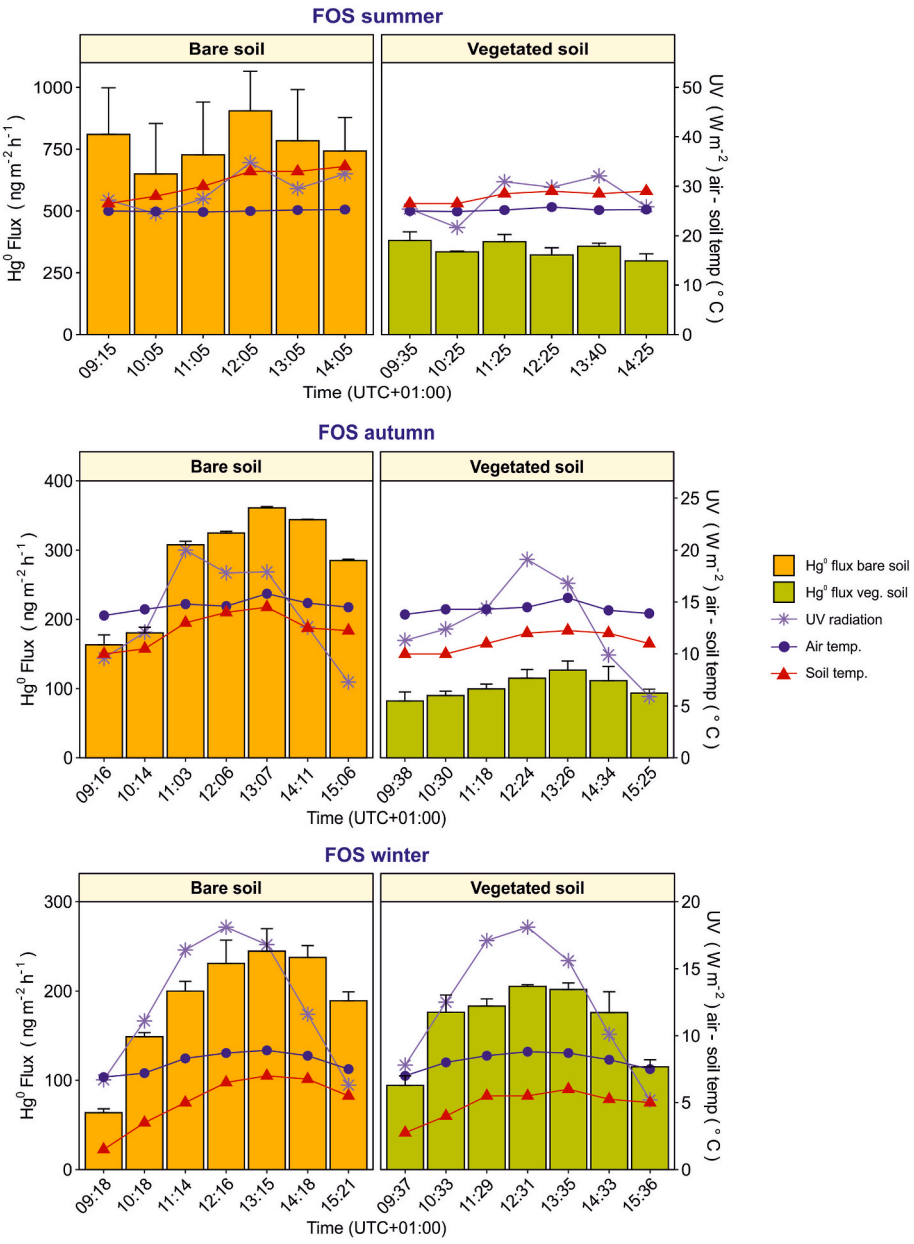

Fig. 4. Example of diurnal variation of Hg^0 fluxes from bare and vegetated soil at site FOS in the various seasons (results from other sites are reported in supplementary material).

This effect was more evident for bare soils and could also be related to progressive soil drying observed in the field, as water evaporation can enhance Hg transport to the surface and its subsequent release (Briggs and Gustin, 2013). A better agreement between patterns of Hg^0 fluxes and soil temperatures was generally observed in autumn and winter than in summer coupled with relatively higher soil moisture, possibly confirming that thermal effects on Hg emissions are more relevant in wet rather than dry soils (Park et al., 2014; Zhou et al., 2017). This is likely related to an increase desorption of bound Hg at a relatively high soil water contents due to the competition of more polar water molecules for binding sites and decreasing binding energy (Briggs and Gustin, 2013; Park et al., 2014). Moreover, increasing water content could also stimulate microbial processes leading to Hg desorption from surfaces (Pannu et al., 2014). Desorbed Hg^{2+} is more available for reduction to Hg^0, a reaction further enhanced at a relatively high soil moisture through the decreasing of soil redox potential (Schlüter, 2000), but this effect has been observed only for relatively high soil water contents (>30% Zhou et al., 2017; MacSween and Edwards, 2021) as most of those observed in our study in autumn and winter (Fig. S3). Temperature increase under such conditions can further enhance the rate of these reactions and favour the transport of both Hg^{2+} and Hg^0 to the soil surface together with water evaporation and the subsequent release of Hg^0 to the atmosphere (Briggs and Gustin, 2013; O'Connor et al., 2019).

Despite low temperatures, Hg^0 fluxes recorded in winter were generally comparable to those found in autumn, particularly in the case of vegetated soil plots likely due to changes in vegetation cover (see Section 3.4.2). During winter, the soil was generally covered by frost in the morning and then gradually thawed. In the first measurements conducted under conditions of low irradiation and temperatures, Hg^0 emissions were generally low, close to the chamber blank, and then sharply increased during the rest of the day. While soil thaws during the day, the contraction of the frozen liquid fraction of the soil matrix can connect the interstitial pore spaces, favouring the movement of Hg^0 potentially stored in soil pore air to the surface (Ci et al., 2018)

particularly at relatively high soil water content (Corbett-Hains et al., 2012) such as those observed in this study in winter, explaining the observed patterns of Hg^0 fluxes. Furthermore, in a recent laboratory study, Walters et al. (2016) observed increasing Hg^0 emission from soils thawing at a constant temperature of around 0 °C and related this increase to the energy transfer to the system rather than changes in temperature. The results of our study appear to be in agreement with this hypothesis, as winter measurements were characterised by relatively high insolation and small changes in soil temperatures during the morning. This effect could explain the occurrence of positive fluxes in winter with soil temperatures near 0 °C, but these low values still limited absolute Hg^0 emission, considering that Hg^0 winter fluxes at SCZ, SVI, and TUR from bare soil plots were significantly ($p < 0.05$, K–W) lower than those recorded in autumn.

3.4.2. *Effects of grass-vegetation cover*

In general, Hg^0 fluxes from grass-vegetated soils were lower than those calculated for bare soils at the same site: considering the daily averages, the vegetation cover caused a reduction of Hg^0 releases compared to bare soil plots of 9.3–68.2% in summer, 41.4–78.0% in autumn, and 12.4–60.0% in winter (Fig. 5). The presence of vegetation influences the environmental variables at the soil-air interface through affecting air mixing, reducing solar radiation that reaches the surface and consequently influencing soil temperature and moisture (Gustin et al., 2004). Through these effects, the presence of vegetation often limits the formation and volatilisation of Hg^0 from soils compared to non-vegetated areas (Agnan et al., 2016; Choi and Holsen, 2009b; Zhang et al., 2021). Lower Hg^0 fluxes from grass-covered as compared to bare soils have been previously reported for areas directly impacted by Hg mining activity (Fantozzi et al., 2013) or waste disposal (Tao et al., 2017), confirming the role of vegetation in reducing the impact of substrate pollution on the local atmosphere (Yan et al., 2019), but also for background zones (Fu et al., 2008; Sun et al., 2020b). However, it should be stressed that Hg^0 fluxes from soils characterised by the presence of vegetation are still regulated by the combined influence of radiation and temperature (Ma et al., 2018; Osterwalder et al., 2019), as also confirmed by the similar trends of emission, UV radiation, and soil temperatures recorded in this study (Fig. 4 and Figs. S6–S10).

Another important aspect that should be considered is the vegetation growth stage, which can seriously control the Hg^0 releases at the soil-air interface (Gao et al., 2020), as typically the reduction of Hg^0 fluxes is higher during active growth and peak vegetation periods and decreases during senescence (Eckley et al., 2021; Sun et al., 2020b). The results obtained in this study are in good agreement with this hypothesis. During summer, Hg^0 fluxes from vegetated soils were significantly ($p < 0.05$, K–W, Fig. 3) lower than from bare soils at sites SVI, SAG, TUR, and FOS, where vegetation was well developed ensuring effective shading and limiting photoreduction and energy reaching the soil surface (Gao et al., 2019). Conversely, measurements at SAV and SCZ were conducted after mowing and removing grass and consequently the shading effect was limited, as confirmed by values of soil temperatures comparable to those found for bare soils. Hence, Hg^0 fluxes, enhanced by higher radiation reaching the surface, were lower but comparable to those found for bare soils, as commonly observed after harvest in agricultural soils (Sommar et al., 2016; Zhu et al., 2011). In autumn, despite a lower vegetation growth, Hg^0 emissions from vegetated plots were found to be significantly lower than those from bare soils at all sites (Fig. 3), suggesting that the physical structure of plants may still have limited the gaseous exchange through reducing light penetration, in agreement with the results of a previous study conducted in pristine meadows (Converse et al., 2010). Finally, in winter Hg^0 fluxes from vegetated soils were comparable and in some cases (SVI, SAV, SCZ, FOS) slightly higher than those found in autumn despite the lower temperatures, likely due to the presence of dry plant stubble which allowed for an increase in light that could reach the soil surface and consequently the formation of Hg^0, as already noted in other studies (Converse et al., 2010; Sun et al., 2020b). Interestingly, Hg^0 fluxes recorded from vegetated soils at site FOS in winter were significantly ($p < 0.05$, K–W) higher than those observed in autumn at the same site, likely due to the combination of scarce vegetation cover during winter and relatively high UV irradiation, as measurements in autumn were conducted under partial cloud cover. Winter conditions with dormant vegetation likely represent soil fluxes with minimal vegetation effects, with emissions that can be comparable to those from bare soils (Stamenkovic et al., 2008), as generally occurred in this study (Fig. 3). Moreover, in some morning measurements during winter slightly higher Hg^0 fluxes from vegetated than bare soils were detected (Fig. 4, S6-S8, S10), pointing to the extremely high uncertainty of the estimation of average Hg^0 flux reduction from vegetated soil plots in winter (Fig. 5): consequently, despite average daily Hg^0 fluxes from vegetated soils in winter being lower than those from bare soils, it is possible to assume that these differences are only marginally related to the presence of vegetation during this season (During et al., 2009). These results confirm that favouring the growth of vegetation on contaminated substrates could represent a simple and inexpensive remediation strategy to reduce Hg^0 releases into the atmosphere, mostly at sites where the local climate allows for the presence of dense natural vegetation during the hottest months of the year, when the highest emissions are expected. However, the efficacy of this strategy should be evaluated considering the local characteristics of each site, as the occurrence of periods with low vegetation development corresponding to high irradiation and temperature could significantly affect the reduction of Hg^0 emissions from soils by vegetation due to lack of soil cover, as observed at SAV and SCZ during summer in this study. For example, this situation could be caused by droughts events, the frequency of which is expected to increase due to global warming: this aspect should be considered when assessing the possible use of this mitigation strategy for Hg-contaminated sites (Zhao and Running, 2010; Jiskra et al., 2018).

On ecosystem level, living plants could also limit the amount of Hg

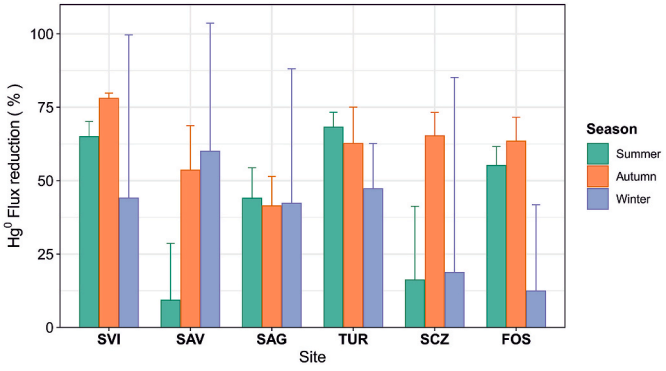

Fig. 5. Estimation of daily average Hg^0 fluxes reduction from grass-vegetated soil plots compared to bare soil plots in the different sites and seasons.

released to the atmosphere through stomatal uptake of Hg^0 emitted by the soil (Eckley et al., 2016) or cuticolar adsorption (Stamenkovic and Gustin, 2009). These processes are thought to be more effective at high atmospheric Hg concentrations and, more importantly, are reversible, as Hg present in the leaf interior or on the surface can be re-emitted to the atmosphere when ambient conditions change (Fu et al., 2008; Naharro et al., 2020). The experimental setup adopted in this study does not allow for the discrimination of the relative contribution of these processes to Hg^0 releases, but the impact of foliar Hg uptake may be considered negligible compared to shading effects, particularly in grassland ecosystems characterised by low leaf areas (Converse et al., 2010; Gao et al., 2020; Sun et al., 2020b).

As fluxes from bare and vegetated soils were measured on contiguous but different plots, it cannot be excluded that the differences in Hg^0 fluxes may be also related to upper soil horizon characteristics (e.g. porosity, THg concentration), which could be highly variable even over short distances (During et al., 2009; Rinklebe et al., 2009). Considering, however, that vegetated plots showed consistently lower fluxes than bare soils, even when characterised by slightly higher THg contents, it can be assumed that the influence of vegetation (in summer and autumn seasons) is greater than that of soil characteristics. Conversely, the variable Hg content in soils heavily influenced the variability of Hg^0 fluxes between the different sites, as discussed in the next section.

3.4.3. *Effects of soil Hg and organic matter content*

The availability of Hg in surface soils represents one of the most important parameters controlling the magnitude of Hg^0 fluxes into the atmosphere, particularly in Hg-enriched areas (Agnan et al., 2016; Osterwalder et al., 2019), and the results of this study are in good agreement with this evidence. The average Hg^0 fluxes from bare soils were indeed significantly correlated with THg concentrations in topsoils both in summer ($r = 0.95$, $p < 0.01$) and autumn ($r = 0.77$, $p < 0.05$), whereas no relation was found in winter (Fig. 6) likely due to the low emissions recorded at all sites during the mornings. Generally, the differences between average Hg^0 fluxes at different sites in summer and autumn may be explained by the different THg concentrations in soils, whereas in winter the Hg^0 releases were more homogenous. For example, Hg^0 fluxes from both bare and vegetated soils at the most impacted site (TUR) in winter, limited by both low temperatures and tree shading in the afternoon, were not statistically different from those of SAV and SCZ, characterised by the lowest Hg content in the substrate.

Moreover, average Hg^0 fluxes in summer and autumn were also significantly correlated with the concentration of α-HgS (Fig. 6), representing the largely predominant Hg fraction in the selected soils. These

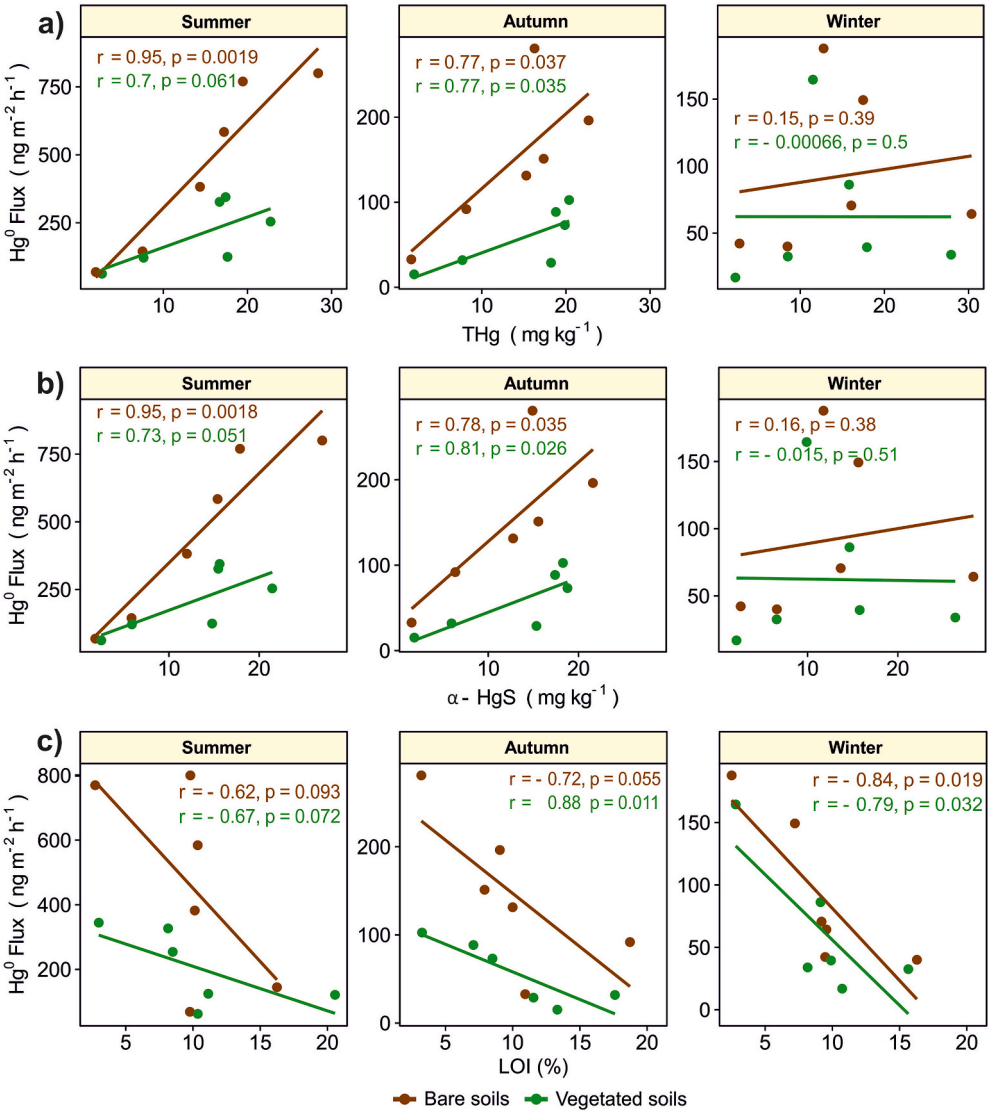

Fig. 6. Correlation between average Hg^0 fluxes from bare and vegetated soils at the experimental sites with a) average soil total Hg concentration b) average soil α-HgS concentration c) average soil OM content (as LOI).

results confirm that despite the low mobility of α-HgS in the environment (Gai et al., 2016), this form can significantly contribute to the releases of Hg^0 from soils likely thanks to the energy provided by irradiation.

The relatively high activation energy required to initiate volatilisation from α-HgS compared to other Hg forms (Gustin et al., 2002; Schlüter, 2000) may also explain the low Hg^0 fluxes recorded during morning measurements in winter coupled with low temperatures. Emissions recorded in these conditions are likely attributable to the no-α-HgS fraction, present in comparable amounts at all the sites. Indeed, Hg forms occurring in this fraction are generally more mobile than α-HgS and could generate a more rapid increase in Hg^0 volatilisation in response to light or thermal excitation (Gustin et al., 2002; Kocman and Horvat, 2010; Llanos et al., 2011). Moreover, a greater contribution of α-HgS to Hg^0 formation and volatilisation could also represent the reason why the highest average fluxes during the winter season corresponded to measurements at SAG and FOS sites, characterised by the highest values of both UV radiation and temperatures (Table S3).

Considering the average Hg^0 fluxes from vegetated soil plots, weaker relationships between soil Hg content and Hg^0 releases were observed especially in summer (Fig. 6), confirming the importance of vegetation for Hg^0 emission abatement. A striking example is represented by comparable emissions recorded from vegetated soil at SVI and SCZ in summer despite the difference in THg (17.63 and 7.65 mg kg^{-1}, respectively): as aforementioned, emissions at SCZ may have been enhanced by vegetation cutting, whereas a thriving grass cover limited the emission at SVI (Zhang et al., 2021).

Additionally, Hg^0 fluxes at FOS were generally higher than expected in all seasons and greater than those recorded, for example, at TUR and SAG despite the lower average Hg content in soil and the cloud cover during field sampling in summer. A possible explanation may be found in the different OM content in soils, lower at FOS than at all other sites. Organic matter has a strong affinity for Hg^0 and can therefore effectively adsorb it in the soil pore space, limiting its vertical diffusion and subsequent release into the atmosphere (Fu et al., 2012; Obrist et al., 2014; Yuan et al., 2019). Moreover, the formation of strong covalent bonds between Hg^{2+} and functional groups of OM, particularly those containing reduced sulphur (Reis et al., 2015b), could also influence the amount of Hg available for reduction to Hg^0 and consequently limit gaseous releases (Gao et al., 2020; Yang et al., 2007). The results obtained in this study are in agreement with this hypothesis, as confirmed by the negative relationships generally observed between average values of LOI and Hg^0 fluxes (Fig. 6), confirming that a low content of OM in soil may be conducive for Hg evasion (Llanos et al., 2011). However, further research is needed to assess if this effect could be at least partially ascribed to changes in the type of OM in the soil (not determined in this study), which can also significantly affect Hg mobility (Sysalová et al., 2017).

4. Conclusions

The results of the field measurements presented in this work represent the first direct evidence of Hg^0 releases from the contaminated soils of the Isonzo River alluvial plain, impacted by Hg due to historical extraction activity from the Idrija mining district. Despite the distance from the contamination source, the obtained values were comparable to those reported worldwide for sites impacted by mining, confirming that past supplies of Hg-enriched material still enhance gaseous releases even more than 25 years after the closure of the mine. Overall, Hg^0 emissions were significantly higher during the summer than autumn and winter, which conversely showed comparable values, due to higher incident UV radiation and temperatures that likely promoted the formation of volatile Hg^0.

Mercury content in the soil, mostly occurring as α-HgS, played an important role in influencing the magnitude of Hg^0 fluxes in the different sites, particularly during summer and autumn, whereas emissions in winter were more homogeneous, likely due to a low contribution of α-HgS to volatilisation under low temperature conditions. Moreover, soil organic matter content likely influenced the evasion of Hg^0 to the atmosphere through the adsorption of Hg, too.

Actively growing native grass-vegetation significantly limited Hg^0 emissions during summer and autumn compared to that from bare soils due to soil shading, whereas in winter this effect was not observed due to the presence of only dormant vegetation, ineffectively covering the soil surface. Considering that a remediation of the plain is unlikely due to the spread of contamination over many kilometres, the preservation of the "natural" situation with grass vegetation cover represents a valuable option to limit the amount of Hg^0 releases and thus the impact of substrate Hg-contamination on the local atmosphere and further spatial spreading through atmospheric transport. However, further research is needed to examine the contribution of plants to Hg^0 exchanges in this area.

Having ascertained the existence of relevant diurnal Hg^0 emissions from the selected contaminated soils, further long-term continuous monitoring is needed to better define the diurnal trend of Hg^0 emissions, also taking into consideration the processes occurring during the nocturnal period and evaluating the possible contribution related to dry and wet atmospheric deposition. Furthermore, considering the good response of the accumulation chamber technique to changes in environmental conditions, particularly of incident radiation, and the rapidity of measures (5 min each), this approach could allow for a high number of distinct measures over a short time in different points. Increasing the number of sampling points per area may then allow for a better evaluation of the variability of Hg^0 fluxes on a small spatial scale, and to accurately assess the diffuse emissions of Hg^0 from a selected area. This approach needs also to be tested with regard to risk assessment procedures in contaminated sites, in order to evaluate the potential exposure of local inhabitants to Hg through inhalation after evaporation from soil surfaces. Moreover, it would be desirable to measure Hg^0 fluxes at the soil-air interface in other environments e.g. the croplands that cover a large part of the Isonzo River alluvial plain, where agricultural activities such as ploughing and harvesting cause a marked disturbance of soils and the exposure of bare soil surfaces to direct incident radiation, potentially leading to strong Hg emissions into the atmosphere.

Credit author statement

Federico Floreani: Conceptualization, Methodology, Investigation, Data curation, Formal analysis, Writing – original draft, Writing – review & editing, Visualisation. Valeria Zappella: Investigation, Data curation, Visualisation. Jadran Faganeli: Conceptualization, Validation. Stefano Covelli: Conceptualization, Methodology, Resources, Writing – original draft, Writing – review & editing, Project administration, Supervision.

Funding

This research did not receive any specific grant from funding agencies in the public, commercial, or not-for-profit sectors.

Declaration of competing interest

The authors declare that they have no known competing financial interests or personal relationships that could have appeared to influence the work reported in this paper.

Data availability

Data will be made available on request.

Acknowledgements

This work is part of the Ph.D. thesis written by Federico Floreani at the University of Trieste; the Ph.D. fellowship was founded by PO FRIULI VENEZIA GIULIA-FONDO SOCIALE EUROPEO 2014/2020. The authors are very grateful to Dr. Alessandro Acquavita for his useful suggestions and his support in identifying sampling points. A special thanks to Federico Vito Zotta for his valuable support in sampling operations. Karry Close is warmly acknowledged for proofreading the manuscript. The two anonymous reviewers are warmly acknowledged for their thorough reviews and useful suggestions which improved the earlier version of the manuscript.

References

Acquavita, A., Brandolin, D., Cattaruzza, C., Felluga, A., Maddaleni, P., Meloni, C., Pasquon, M., Predonzani, S., Poli, L., Skert, N., Zanello, A., 2022. Mercury distribution and speciation in historically contaminated soils of the Isonzo River Plain (NE Italy). J. Soils Sediments 22, 79–92. https://doi.org/10.1007/s11368-021-03038-2.

Agnan, Y., Le Dantec, T., Moore, C.W., Edwards, G.C., Obrist, D., 2016. New constraints on terrestrial surface-atmosphere fluxes of gaseous elemental mercury using a global database. Environ. Sci. Technol. 50, 507–524. https://doi.org/10.1021/acs.est.5b04013.

Anderson, A., 1979. Mercury in Soils. In: Nriagu, J.O. (Ed.), The Biogeochemistry of Mercury in the Environment. Elsevier/North Holland, Amsterdam, pp. 79–112.

ARPA FVG-OSMER e GRN, 2021. Database "OMNIA". Available online: http://www.meteo.fvg.it/. (Accessed 27 September 2022).

Bagnato, E., Barra, M., Cardellini, C., Chiodini, G., Parello, F., Sprovieri, M., 2014. First combined flux chamber survey of mercury and CO2 emissions from soil diffuse degassing at Solfatara of Pozzuoli crater, Campi Flegrei (Italy): mapping and quantification of gas release. J. Volcanol. Geoth. Res. 289, 26–40. https://doi.org/10.1016/j.jvolgeores.2014.10.017.

Bahlmann, E., Ebinghaus, R., Ruck, W., 2006. Development and application of a laboratory flux measurement system (LFMS) for the investigation of the kinetics of mercury emissions from soils. J. Environ. Manag. 81, 114–125. https://doi.org/10.1016/j.jenvman.2005.09.022.

Baptista-Salazar, C., Richard, J.H., Horf, M., Rejc, M., Gosar, M., Biester, H., 2017. Grain-size dependence of mercury speciation in river suspended matter, sediments and soils in a mercury mining area at varying hydrological conditions. Appl. Geochem. 81, 132–142. https://doi.org/10.1016/j.apgeochem.2017.04.006.

Barago, N., Floreani, F., Acquavita, A., Esbrí, J.M., Covelli, S., Higueras, P., 2020. Spatial and temporal trends of gaseous elemental mercury over a highly impacted coastal environment (Northern Adriatic, Italy). Atmosphere (Basel) 11, 935. https://doi.org/10.3390/atmos11090935.

Bavec, Š., Gosar, M., 2016. Speciation, mobility and bioaccessibility of Hg in the polluted urban soil of Idrija (Slovenia). Geoderma 273, 115–130. https://doi.org/10.1016/j.geoderma.2016.03.015.

Beckers, F., Rinklebe, J., 2017. Cycling of mercury in the environment: sources, fate, and human health implications: a review. Crit. Rev. Environ. Sci. 47, 693–794. https://doi.org/10.1080/10643389.2017.1326277.

Berg, T., Aspmo, K., Steinnes, E., 2008. Transport of Hg from Atmospheric mercury depletion events to the mainland of Norway and its possible influence on Hg deposition. Geophys. Res. Lett. 35, L09802 https://doi.org/10.1029/2008GL033586.

Biester, H., Gosar, M., Covelli, S., 2000. Mercury speciation in sediments affected by dumped mining residues in the drainage area of the Idrija mercury mine, Slovenia. Environ. Sci. Technol. 34, 3330–3336. https://doi.org/10.1021/es991334v.

Biester, H., Scholz, C., 1997. Determination of mercury binding forms in contaminated soils: mercury pyrolysis versus sequential extractions. Environ. Sci. Technol. 31, 233–239. https://doi.org/10.1021/es960369h.

Boening, D.W., 2000. Ecological effects, transport, and fate of mercury: a general review. Chemosphere 40, 1335–1351. https://doi.org/10.1016/S0045-6535(99)00283-0.

Bourdineaud, J.P., Durn, G., Režun, B., Manceau, A., Hrenović, J., 2020. The chemical species of mercury accumulated by Pseudomonas idrijaensis, a bacterium from a rock of the Idrija mercury mine, Slovenia. Chemosphere 248, 126002. https://doi.org/10.1016/j.chemosphere.2020.126002.

Briggs, C., Gustin, M.S., 2013. Building upon the conceptual model for soil mercury flux: evidence of a link between moisture evaporation and Hg evasion. Water, Air, Soil Pollut. 224, 1744. https://doi.org/10.1007/s11270-013-1744-5.

Cabassi, J., Venturi, S., Di Bennardo, F., Nisi, B., Tassi, F., Magi, F., Ricci, A., Picchi, G., Vaselli, O., 2021. Flux measurements of gaseous elemental mercury (GEM) from the geothermal area of "Le Biancane" natural park (Monterotondo Marittimo, Grosseto, Italy): biogeochemical processes controlling GEM emission. J. Geochem. Explor. 228, 106824 https://doi.org/10.1016/j.gexplo.2021.106824.

Camarda, M., Gurrieri, S., Valenza, M., 2009. Effects of soil permeability and recirculation flux on soil CO_2 flux measurements performed using a closed dynamic accumulation chamber. Chem. Geol. 265, 387–393. https://doi.org/10.1016/j.chemgeo.2009.05.002.

Campos-Guillén, J., Pérez, J.C., Medina, J.A.C., Vera, C.M., Rosas, L.M.S., Gutiérrez, C.L., Salinas, I.G., Hernández Ramírez, M.R., Alonso, G.S., Hernández, A.C., Gutiérrez, C. S., Gómez, S.R., Martínez, X.P., Hidalgo, E., álvarez, Gosar, M., Dizdarevič, T., 2014. Draft genome sequence of the mercury-resistant bacterium Acinetobacter idrijaensis strain MII, isolated from a mine-impacted area, Idrija, Slovenia. Genome Announc. 2 https://doi.org/10.1128/genomeA.01177-14.

Carmona, M., Llanos, W., Higueras, P., Kocman, D., 2013. Mercury emissions in equilibrium: a novel approach for the quantification of mercury emissions from contaminated soils. Anal. Methods 5, 2793–2801. https://doi.org/10.1039/c3ay25700b.

Carpi, A., Lindberg, S.E., 1998. Application of a Teflon® dynamic flux chamber for quantifying soil mercury flux: tests and results over background soil. Atmos. Environ. 32, 873–882. https://doi.org/10.1016/S1352-2310(97)00133-7.

Cerovac, A., Covelli, S., Emili, A., Pavoni, E., Petranich, E., Gregorič, A., Urbanc, J., Zavagno, E., Zini, L., 2018. Mercury in the unconfined aquifer of the Isonzo/SoČa River alluvial plain downstream from the Idrija mining area. Chemosphere 195, 749–761. https://doi.org/10.1016/j.chemosphere.2017.12.105.

Chiodini, G., Cioni, R., Guidi, M., Raco, B., Marini, L., 1998. Soil CO2 flux measurements in volcanic and geothermal areas. Appl. Geochem. 13, 543–552. https://doi.org/10.1016/S0883-2927(97)00076-0.

Choi, H.D., Holsen, T.M., 2009a. Gaseous mercury emissions from unsterilized and sterilized soils: the effect of temperature and UV radiation. Environ. Pollut. 157, 1673–1678. https://doi.org/10.1016/j.envpol.2008.12.014.

Choi, H.D., Holsen, T.M., 2009b. Gaseous mercury fluxes from the forest floor of the Adirondacks. Environ. Pollut. 157, 592–600. https://doi.org/10.1016/j.envpol.2008.08.020.

Ci, Z., Peng, F., Xue, X., Zhang, X., 2018. Temperature sensitivity of gaseous elemental mercury in the active layer of the Qinghai-Tibet Plateau permafrost. Environ. Pollut. 238, 508–515. https://doi.org/10.1016/j.envpol.2018.02.085.

Ci, Z., Peng, F., Xue, X., Zhang, X., 2016. Air-surface exchange of gaseous mercury over permafrost soil: an investigation at a high-altitude (4700 m.a.s.l.) and remote site in the central Qinghai-Tibet Plateau. Atmos. Chem. Phys. 16, 14741–14754. https://doi.org/10.5194/acp-16-14741-2016.

Clarkson, T.W., Magos, L., 2006. The toxicology of mercury and its chemical compounds. Crit. Rev. Toxicol. 36, 609–662. https://doi.org/10.1080/10408440600845619.

Colica, A., Benvenuti, M., Chiarantini, L., Costagliola, P., Lattanzi, P., Rimondi, V., Rinaldi, M., 2019. From point source to diffuse source of contaminants: the example of mercury dispersion in the Paglia River (Central Italy). Catena 172, 488–500. https://doi.org/10.1016/j.catena.2018.08.043.

Contin, M., Rizzardini, C.B., Catalano, L., De Nobili, M., 2012. Contamination by mercury affects methane oxidation capacity of aerobic arable soils. Geoderma 189–190, 250–256. https://doi.org/10.1016/j.geoderma.2012.06.031.

Converse, A.D., Riscassi, A.L., Scanlon, T.M., 2014. Seasonal contribution of dewfall to mercury deposition determined using a micrometeorological technique and dew chemistry. J. Geophys. Res. 119, 284–292. https://doi.org/10.1002/2013JD020491.

Converse, A.D., Riscassi, A.L., Scanlon, T.M., 2010. Seasonal variability in gaseous mercury fluxes measured in a high-elevation meadow. Atmos. Environ. 44, 2176–2185. https://doi.org/10.1016/j.atmosenv.2010.03.024.

Corbett-Hains, H., Walters, N.E., Van Heyst, B.J., 2012. Evaluating the effects of sub-zero temperature cycling on mercury flux from soils. Atmos. Environ. 63, 102–108. https://doi.org/10.1016/j.atmosenv.2012.09.047.

Cotel, S., Schäfer, G., Traverse, S., Marzougui-Jaafar, S., Gay, G., Razakarisoa, O., 2015. Evaluation of VOC fluxes at the soil-air interface using different flux chambers and a quasi-analytical approach. Water, Air, Soil Pollut. 226, 356. https://doi.org/10.1007/s11270-015-2596-y.

Coufalík, P., Krásenský, P., Dosbaba, M., Komárek, J., 2012. Sequential extraction and thermal desorption of mercury from contaminated soil and tailings from Mongolia. Cent. Eur. J. Chem. 10, 1565–1573. https://doi.org/10.2478/s11532-012-0074-6.

Cucchi, F., Franceschini, G., Zini, L., 2008. Hydrogeochemical investigations and groundwater provinces of the Friuli Venezia Giulia Plain aquifers, northeastern Italy. Environ. Geol. 55, 985–999. https://doi.org/10.1007/s00254-007-1048-4.

Da Lio, C., Tosi, L., 2018. Land subsidence in the Friuli Venezia Giulia coastal plain, Italy: 1992–2010 results from SAR-based interferometry. Sci. Total Environ. 633, 752–764. https://doi.org/10.1016/j.scitotenv.2018.03.244.

Dalziel, J., Tordon, R., 2014. Gaseous mercury flux measurements from two mine tailing sites in the Seal Harbour area of Nova Scotia. Geochem. Explor. Environ. Anal. 14, 17–24. https://doi.org/10.1144/geochem2011-112.

Davidson, E.A., Savage, K., Verchot, L.V., Navarro, R., 2002. Minimizing artifacts and biases in chamber-based measurements of soil respiration. Agric. For. Meteorol. 113, 21–37. https://doi.org/10.1016/S0168-1923(02)00100-4.

Debure, M., Grangeon, S., Robinet, J.C., Madé, B., Fernández, A.M., Lerouge, C., 2020. Influence of soil redox state on mercury sorption and reduction capacity. Sci. Total Environ. 707, 136069 https://doi.org/10.1016/j.scitotenv.2019.136069.

Di Francesco, F., Ferrara, R., Mazzolai, B., 1998. Two ways of using a chamber for mercury flux measurement - a simple mathematical approach. Sci. Total Environ. 213, 33–41. https://doi.org/10.1016/S0048-9697(98)00068-0.

Dizdarevič, T., 2001. The influence of mercury production in Idrija mine on the environment in the Idrija region and over a broad area. RMZ Mater. Geoenviron 48, 56–64.

Douglas, T.A., Blum, J.D., 2019. Mercury isotopes reveal atmospheric gaseous mercury deposition directly to the arctic coastal snowpack. Environ. Sci. Technol. Lett. 6, 235–242. https://doi.org/10.1021/acs.estlett.9b00131.

During, A., Rinklebe, J., Böhme, F., Wennrich, R., Stärk, H.J., Mothes, S., Du Laing, G., Schulz, E., Neue, H.U., 2009. Mercury volatilization from three floodplain soils at the Central Elbe River, Germany. Soil Sediment Contam. 18, 429–444. https://doi.org/10.1080/15320380902962395.

Eckley, C.S., Blanchard, P., McLennan, D., Mintz, R., Sekela, M., 2015. Soil-air mercury flux near a large industrial emission source before and after closure (flin flon, manitoba, Canada). Environ. Sci. Technol. 49, 9750–9757. https://doi.org/10.1021/acs.est.5b01995.

Eckley, C.S., Eagles-Smith, C., Tate, M.T., Krabbenhoft, D.P., 2021. Surface-air mercury fluxes and a watershed mass balance in forested and harvested catchments. Environ. Pollut. 277, 116869 https://doi.org/10.1016/j.envpol.2021.116869.

Eckley, C.S., Tate, M.T., Lin, C.J., Gustin, M., Dent, S., Eagles-Smith, C., Lutz, M.A., Wickland, K.P., Wang, B., Gray, J.E., Edwards, G.C., Krabbenhoft, D.P., Smith, D.B., 2016. Surface-air mercury fluxes across Western North America: a synthesis of spatial trends and controlling variables. Sci. Total Environ. 568, 651–665. https://doi.org/10.1016/j.scitotenv.2016.02.121.

Esbrí, J.M., Bernaus, A., Ávila, M., Kocman, D., García-Noguero, E.M., Guerrero, B., Gaona, X., Álvarez, R., Perez-Gonzalez, G., Valiente, M., Higueras, P., Horvat, M., Loredo, J., 2010. XANES speciation of mercury in three mining districts - almadén, Asturias (Spain), Idria (Slovenia). J. Synchrotron Radiat. 17, 179–186. https://doi.org/10.1107/S0909049510001925.

Fantozzi, L., Ferrara, R., Dini, F., Tamburello, L., Pirrone, N., Sprovieri, F., 2013. Study on the reduction of atmospheric mercury emissions from mine waste enriched soils through native grass cover in the Mt. Amiata region of Italy. Environ. Res. 125, 69–74. https://doi.org/10.1016/j.envres.2013.02.004.

Ferrari, C.P., Padova, C., Faïn, X., Gauchard, P.A., Dommergue, A., Aspmo, K., Berg, T., Cairns, W., Barbante, C., Cescon, P., Kaleschke, L., Richter, A., Wittrock, F., Boutron, C., 2008. Atmospheric mercury depletion event study in Ny-Alesund (Svalbard) in spring 2005. Deposition and transformation of Hg in surface snow during springtime. Sci. Total Environ. 397, 167–177. https://doi.org/10.1016/j.scitotenv.2008.01.064.

Floreani, F., Barago, N., Acquavita, A., Covelli, S., Skert, N., Higueras, P., 2020. Spatial distribution and biomonitoring of atmospheric mercury concentrations over a contaminated coastal lagoon (Northern Adriatic, Italy). Atmosphere (Basel) 11, 1280. https://doi.org/10.3390/atmos11121280.

Fontana, A., Mozzi, P., Bondesan, A., 2008. Alluvial megafans in the Venetian-Friulian plain (north-eastern Italy): evidence of sedimentary and erosive phases during late pleistocene and holocene. Quat. Int. 189, 71–90. https://doi.org/10.1016/j.quaint.2007.08.044.

Fritsche, J., Obrist, D., Alewell, C., 2008. Evidence of microbial control of Hg0 emissions from uncontaminated terrestrial soils. J. Plant Nutr. Soil Sci. 171, 200–209. https://doi.org/10.1002/jpln.200625211.

Fu, X., Feng, X., Wang, S., 2008. Exchange fluxes of Hg between surfaces and atmosphere in the eastern flank of Mount Gongga, Sichuan province, southwestern China. J. Geophys. Res. Atmos. 113, D20306 https://doi.org/10.1029/2008JD009814.

Fu, X., Feng, X., Zhang, H., Yu, B., Chen, L., 2012. Mercury emissions from natural surfaces highly impacted by human activities in Guangzhou province, South China. Atmos. Environ. 54, 185–193. https://doi.org/10.1016/j.atmosenv.2012.02.008.

Gabriel, M.C., Williamson, D.G., 2004. Principal biogeochemical factors affecting the speciation and transport of mercury through the terrestrial environment. Environ. Geochem. Health 26, 421–434. https://doi.org/10.1007/s10653-004-1308-0.

Gai, K., Hoelen, T.P., Hsu-Kim, H., Lowry, G.V., 2016. Mobility of four common mercury species in model and natural unsaturated soils. Environ. Sci. Technol. 50, 3342–3351. https://doi.org/10.1021/acs.est.5b04247.

Gao, Y., Wang, Z., Wang, C., Zhang, X., 2019. The soil displacement measurement of mercury emission flux of the sewage irrigation farmlands in Northern China. Ecosys. Health Sustain. 5, 169–180. https://doi.org/10.1080/20964129.2019.1647117.

Gao, Y., Wang, Z., Zhang, X., Wang, C., 2020. Observation and estimation of mercury exchange fluxes from soil under different crop cultivars and planting densities in North China Plain. Environ. Pollut. 259, 113833 https://doi.org/10.1016/j.envpol.2019.113833.

García-Sánchez, A., Contreras, F., Adams, M., Santos, F., 2006. Atmospheric mercury emissions from polluted gold mining areas (Venezuela). Environ. Geochem. Health 28, 529–540. https://doi.org/10.1007/s10653-006-9049-x.

Giaiotti, D., Nordio, S., Stel, F., 2003. The climatology of hail in the plain of Friuli Venezia Giulia. Atmos. Res. 67–68, 247–259. https://doi.org/10.1016/S0169-8095(03)00084-X.

Gilli, R.S., Karlen, C., Weber, M., Rüegg, J., Barmettler, K., Biester, H., Boivin, P., Kretzschmar, R., 2018. Speciation and mobility of mercury in soils contaminated by legacy emissions from a chemical factory in the rhône valley in canton of valais, Switzerland. Soil Syst 2, 44. https://doi.org/10.3390/soilsystems2030044.

Gillis, A., Miller, D.R., 2000. Some potential errors in the measurement of mercury gas exchange at the soil surface using a dynamic flux chamber. Sci. Total Environ. 260, 181–189. https://doi.org/10.1016/S0048-9697(00)00562-3.

Gosar, M., Pirc, S., Bidovec, M., 1997. Mercury in the Idrijca River sediments as a reflection of mining and smelting activities of the Idrija mercury mine. J. Geochem. Explor. 58, 125–131. https://doi.org/10.1016/S0375-6742(96)00064-7.

Gustin, M.S., Biester, H., Kim, C.S., 2002. Investigation of the light-enhanced emission of mercury from naturally enriched substrates. Atmos. Environ. 36, 3241–3254. https://doi.org/10.1016/S1352-2310(02)00329-1.

Gustin, M.S., Coolbaugh, M.F., Engle, M.A., Fitzgerald, B.C., Keislar, R.E., Lindberg, S.E., Nacht, D.M., Quashnick, J., Rytuba, J.J., Sladek, C., Zhang, H., Zehner, R.E., 2003. Atmospheric mercury emissions from mine wastes and surrounding geologically enriched terrains. Environ. Geol. 43, 339–351. https://doi.org/10.1007/s00254-002-0630-z.

Gustin, M.S., Ericksen, J.A., Schorran, D.E., Johnson, D.W., Lindberg, S.E., Coleman, J.S., 2004. Application of controlled mesocosms for understanding mercury air-soil-plant exchange. Environ. Sci. Technol. 38, 6044–6050. https://doi.org/10.1021/es0487933.

Heiri, O., Lotter, A.F., Lemcke, G., 2001. Loss on ignition as a method for estimating organic and carbonate content in sediments: reproducibility and comparability of results. J. Paleolimnol. 25, 101–110. https://doi.org/10.1023/A:1008119611481.

Hines, M.E., Horvat, M., Faganeli, J., Bonzongo, J.C.J., Barkay, T., Major, E.B., Scott, K.J., Bailey, E.A., Warwick, J.J., Lyons, W.B., 2000. Mercury biogeochemistry in the idrija river, Slovenia, from above the mine into the gulf of trieste. Environ. Res. 83, 129–139. https://doi.org/10.1006/enrs.2000.4052.

Horowitz, H.M., Jacob, D.J., Zhang, Y., Dibble, T.S., Slemr, F., Amos, H.M., Schmidt, J.A., Corbitt, E.S., Marais, E.A., Sunderland, E.M., 2017. A new mechanism for atmospheric mercury redox chemistry: implications for the global mercury budget. Atmos. Chem. Phys. 17, 6353–6371. https://doi.org/10.5194/acp-17-6353-2017.

Hutchinson, G.L., Livingston, G.P., 2001. Vents and seals in non-steady-state chambers used for measuring gas exchange between soil and the atmosphere. Eur. J. Soil Sci. 52, 675–682. https://doi.org/10.1046/j.1365-2389.2001.00415.x.

ISO 13320:2020, 2020. Particle Size Analysis - Laser Diffraction Methods, second ed. 01, Geneva.

Jiskra, M., Sonke, J.E., Obrist, D., Bieser, J., Ebinghaus, R., Myhre, C.L., Pfaffhuber, K.A., Wängberg, I., Kyllönen, K., Worthy, D., Martin, L.G., Labuschagne, C., Mkololo, T., Ramonet, M., Magand, O., Dommergue, A., 2018. A vegetation control on seasonal variations in global atmospheric mercury concentrations. Nat. Geosci. 11, 244–250. https://doi.org/10.1038/s41561-018-0078-8.

Jiskra, M., Wiederhold, J.G., Skyllberg, U., Kronberg, R.M., Hajdas, I., Kretzschmar, R., 2015. Mercury deposition and Re-emission pathways in boreal forest soils investigated with Hg isotope signatures. Environ. Sci. Technol. 49, 7188–7196. https://doi.org/10.1021/acs.est.5b00742.

Kandel, T.P., Lærke, P.E., Elsgaard, L., 2016. Effect of chamber enclosure time on soil respiration flux: a comparison of linear and non-linear flux calculation methods. Atmos. Environ. 141, 245–254. https://doi.org/10.1016/j.atmosenv.2016.06.062.

Kocman, D., Horvat, M., 2010. A laboratory based experimental study of mercury emission from contaminated soils in the River Idrijca catchment. Atmos. Chem. Phys. 10, 1417–1426. https://doi.org/10.5194/acp-10-1417-2010.

Kocman, D., Horvat, M., Pirrone, N., Cinnirella, S., 2013. Contribution of contaminated sites to the global mercury budget. Environ. Res. 125, 160–170. https://doi.org/10.1016/j.envres.2012.12.011.

Kotnik, J., Horvat, M., Dizdarevič, T., 2005. Current and past mercury distribution in air over the Idrija Hg mine region, Slovenia. Atmos. Environ. 39, 7570–7579. https://doi.org/10.1016/j.atmosenv.2005.06.061.

Kurz, A.Y., Blum, J.D., Washburn, S.J., Baskaran, M., 2019. Changes in the mercury isotopic composition of sediments from a remote alpine lake in Wyoming. USA. Sci. Total Environ. 669, 973–982. https://doi.org/10.1016/j.scitotenv.2019.03.165.

Kyllönen, K., Hakola, H., Hellén, H., Korhonen, M., Verta, M., 2012. Atmospheric mercury fluxes in a southern boreal forest and wetland. Water, Air, Soil Pollut. 223, 1171–1182. https://doi.org/10.1007/s11270-011-0935-1.

Lei, D., Xiaohui, S., Yao, L., Baoyu, D., Qiong, W., Kaiyun, L., Jiawei, Z., Qingru, W., Shuxiao, W., 2021. Soil-atmosphere exchange of gaseous elemental mercury in three subtropical forests with different substrate Hg concentrations. Atmos. Environ. 244, 117869 https://doi.org/10.1016/j.atmosenv.2020.117869.

Li, C., Liang, H., Liang, M., Chen, Y., Zhou, Y., 2018. Mercury emissions flux from various land uses in old mining area, Inner Mongolia, China. J. Geochem. Explor. 192, 132–141. https://doi.org/10.1016/j.gexplo.2018.06.011.

Liu, F., Cheng, H., Yang, K., Zhao, C., Liu, Y., Peng, M., Li, K., 2014. Characteristics and influencing factors of mercury exchange flux between soil and air in Guangzhou City. J. Geochem. Explor. 139, 115–121. https://doi.org/10.1016/j.gexplo.2013.09.005.

Llanos, W., Kocman, D., Higueras, P., Horvat, M., 2011. Mercury emission and dispersion models from soils contaminated by cinnabar mining and metallurgy. J. Environ. Monit. 13, 3460–3468. https://doi.org/10.1039/c1em10694e.

Ma, M., Sun, T., Du, H., Wang, D., 2018. A two-year study on mercury fluxes from the soil under different vegetation cover in a subtropical region, South China. Atmosphere (Basel) 9, 30. https://doi.org/10.3390/atmos9010030.

MacSween, K., Edwards, G.C., 2021. The role of precipitation and soil moisture in enhancing mercury air-surface exchange at a background site in south-eastern Australia. Atmos. Environ. 255, 118445 https://doi.org/10.1016/j.atmosenv.2021.118445.

Mahbub, K.R., Krishnan, K., Megharaj, M., Naidu, R., 2016. Bioremediation potential of a highly mercury resistant bacterial strain Sphingobium SA2 isolated from contaminated soil. Chemosphere 144, 330–337. https://doi.org/10.1016/j.chemosphere.2015.08.061.

Maier, M., Weber, T.K.D., Fiedler, J., Fuß, R., Glatzel, S., Huth, V., Jordan, S., Jurasinski, G., Kutzbach, L., Schäfer, K., Weymann, D., Hagemann, U., 2022. Introduction of a guideline for measurements of greenhouse gas fluxes from soils using non-steady-state chambers. J. Plant Nutr. Soil Sci. 185, 447–461. https://doi.org/10.1002/jpln.202200199.

Marocco, R., 1989. Lineamenti geomorfologici della costa e dei fondali del Golfo di Trieste e considerazioni sulla loro evoluzione Tardo-Quaternaria. Int. J. Speleol. 18, 87–110. https://doi.org/10.5038/1827-806x.18.3.2.

Marsik, F.J., Keeler, G.J., Lindberg, S.E., Zhang, H., 2005. Air-surface exchange of gaseous mercury over a mixed sawgrass-cattail stand within the Florida Everglades. Environ. Sci. Technol. 39, 4739–4746. https://doi.org/10.1021/es0404015.

Mashyanov, N.R., Pogarev, S.E., Panova, E.G., Panichev, N., Ryzhov, V., 2017. Determination of mercury thermospecies in coal. Fuel 203, 973–980. https://doi.org/10.1016/j.fuel.2017.03.085.

Mathema, V.B., Thakuri, B.C., Sillanpää, M., 2011. Bacterial mer operon-mediated detoxification of mercurial compounds: a short review. Arch. Microbiol. 193, 837–844. https://doi.org/10.1007/s00203-011-0751-4.
Miller, M.B., Gustin, M.S., Eckley, C.S., 2011. Measurement and scaling of air-surface mercury exchange from substrates in the vicinity of two Nevada gold mines. Sci. Total Environ. 409, 3879–3886. https://doi.org/10.1016/j.scitotenv.2011.05.040.
Moore, C., Carpi, A., 2005. Mechanisms of the emission of mercury from soil: role of UV radiation. J. Geophys. Res. Atmos. 110, D24302 https://doi.org/10.1029/2004JD005567.
Naharro, R., Esbrí, J.M., Amorós, J.A., Higueras, P.L., 2020. Experimental assessment of the daily exchange of atmospheric mercury in Epipremnum aureum. Environ. Geochem. Health 42, 3185–3198. https://doi.org/10.1007/s10653-020-00557-8.
O'Connor, D., Hou, D., Ok, Y.S., Mulder, J., Duan, L., Wu, Q., Wang, S., Tack, F.M.G., Rinklebe, J., 2019. Mercury speciation, transformation, and transportation in soils, atmospheric flux, and implications for risk management: a critical review. Environ. Int. 126, 747–761. https://doi.org/10.1016/j.envint.2019.03.019.
Obrist, D., Pokharel, A.K., Moore, C., 2014. Vertical profile measurements of soil air suggest immobilization of gaseous elemental mercury in mineral soil. Environ. Sci. Technol. 48, 2242–2252. https://doi.org/10.1021/es4048297.
Osterwalder, S., Huang, J.H., Shetaya, W.H., Agnan, Y., Frossard, A., Frey, B., Alewell, C., Kretzschmar, R., Biester, H., Obrist, D., 2019. Mercury emission from industrially contaminated soils in relation to chemical, microbial, and meteorological factors. Environ. Pollut. 250, 944–952. https://doi.org/10.1016/j.envpol.2019.03.093.
Ottesen, R.T., Birke, M., Finne, T.E., Gosar, M., Locutura, J., Reimann, C., Tarvainen, T., Albanese, S., Andersson, M., Arnoldussen, A., Batista, M.J., Bel-lan, A., Cicchella, D., Demetriades, A., Dinelli, E., De Vivo, B., De Vos, W., Duris, M., Dusza, A., Eggen, O. A., Eklund, M., Ernstsen, V., Filzmoser, P., Flight, D., Fuchs, M., Fugedi, U., Gilucis, A., Gregorauskiene, V., Gulan, A., Halamić, J., Haslinger, E., Hayoz, P., Hoffmann, R., Hoogewerff, J., Hrvatovic, H., Husnjak, S., Johnson, C.C., Jordan, G., Kaste, L., Keilert, B., Kivisilla, J., Klos, V., Krone, F., Kwecko, P., Kuti, L., Ladenberger, A., Lima, A., Lucivjansky, D.P., Mackovych, D., Malyuk, B.I., Maquil, R., McDonnell, P., Meuli, R.G., Miosic, N., Mol, G., Négrel, P., O'Connor, P., Pasieczna, A., Petersell, W., Poňavič, M., Pramuka, S., Prazeres, C., Rauch, U., Reitner, H., Sadeghi, M., Salpeteur, I., Samardzic, N., Schedl, A., Scheib, A., Schoeters, I., Sefcik, P., Skopljak, F., Slaninka, I., Šorša, A., Stafilov, T., Sellersjö, E., Trendavilov, V., Valera, P., Verougstraete, V., Vidojević, D., Zomeni, Z., 2013. Mercury in European agricultural and grazing land soils. Appl. Geochem. 33, 1–12. https://doi.org/10.1016/j.apgeochem.2012.12.013.
Palmieri, H.E.L., Nalini, H.A., Leonel, L.V., Windmöller, C.C., Santos, R.C., de Brito, W., 2006. Quantification and speciation of mercury in soils from the tripuí ecological station, minas gerais, Brazil. Sci. Total Environ. 368, 69–78. https://doi.org/10.1016/j.scitotenv.2005.09.085.
Pannu, R., Siciliano, S.D., O'Driscoll, N.J., 2014. Quantifying the effects of soil temperature, moisture and sterilization on elemental mercury formation in boreal soils. Environ. Pollut. 193, 138–146. https://doi.org/10.1016/j.envpol.2014.06.023.
Park, S.Y., Holsen, T.M., Kim, P.R., Han, Y.J., 2014. Laboratory investigation of factors affecting mercury emissions from soils. Environ. Earth Sci. 72, 2711–2721. https://doi.org/10.1007/s12665-014-3177-x.
Pavoni, E., Petranich, E., Signore, S., Fontolan, G., Covelli, S., 2021. The legacy of the idrija mine twenty-five years after closing: is mercury in the water column of the gulf of trieste still an environmental issue? Int. J. Environ. Res. Publ. Health 18, 10192. https://doi.org/10.3390/ijerph181910192.
Pelcová, P., Ridošková, A., Hrachovinová, J., Grmela, J., 2021. Evaluation of mercury bioavailability to vegetables in the vicinity of cinnabar mine. Environ. Pollut. 283, 117092 https://doi.org/10.1016/j.envpol.2021.117092.
Petranich, E., Predonzani, S., Acquavita, A., Mashyanov, N., Covelli, S., 2022. Applied Geochemistry Rapid thermoscanning technique for direct analysis of mercury species in contaminated sediments : from pure compounds to real sample application. Appl. Geochem. 143, 105393 https://doi.org/10.1016/j.apgeochem.2022.105393.
Piani, A., Acquavita, A., Catalano, L., Contin, M., Mattassi, G., De Nobili, M., 2013. Effects of long term Hg contamination on soil mercury speciation and soil biological activities. E3S Web Conf. 1, 1–4. https://doi.org/10.1051/e3sconf/20130108001.
Pirrone, N., Cinnirella, S., Feng, X., Finkelman, R.B., Friedli, H.R., Leaner, J., Mason, R., Mukherjee, A.B., Stracher, G.B., Streets, D.G., Telmer, K., 2010. Global mercury emissions to the atmosphere from anthropogenic and natural sources. Atmos. Chem. Phys. 10, 5951–5964. https://doi.org/10.5194/acp-10-5951-2010.
Reis, A.T., Coelho, J.P., Rucandio, I., Davidson, C.M., Duarte, A.C., Pereira, E., 2015a. Thermo-desorption: a valid tool for mercury speciation in soils and sediments? Geoderma 237, 98–104. https://doi.org/10.1016/j.geoderma.2014.08.019.
Reis, A.T., Lopes, C.B., Davidson, C.M., Duarte, A.C., Pereira, E., 2015b. Extraction of available and labile fractions of mercury from contaminated soils: the role of operational parameters. Geoderma 259–260, 213–223. https://doi.org/10.1016/j.geoderma.2015.06.004.
Rinklebe, J., During, A., Overesch, M., Du Laing, G., Wennrich, R., Stärk, H.J., Mothes, S., 2010. Dynamics of mercury fluxes and their controlling factors in large Hg-polluted floodplain areas. Environ. Pollut. 158, 308–318. https://doi.org/10.1016/j.envpol.2009.07.001.
Rinklebe, J., During, A., Overesch, M., Wennrich, R., Stärk, H.J., Mothes, S., Neue, H.U., 2009. Optimization of a simple field method to determine mercury volatilization from soils-Examples of 13 sites in floodplain ecosystems at the Elbe River (Germany). Ecol. Eng. 35, 319–328. https://doi.org/10.1016/j.ecoleng.2008.04.019.
Rivas-Martínez, S., Rivas-Sáenz, S., Penas-Merino, A., 2011. Worldwide bioclimatic classification system. Glob. Geobot. 1, 1–638. https://doi.org/10.1127/0340-269X/2006.
Rochette, P., Hutchinson, G.L., 2005. Measurement of Soil Respiration in Situ: Chamber Techniques. In: Micrometeorology in Agricultural Systems. John Wiley & Sons, Ltd, pp. 247–286. https://doi.org/10.2134/agronmonogr47.c12.
Rumayor, M., Gallego, J.R., Rodríguez-Valdés, E., Díaz-Somoano, M., 2017. An assessment of the environmental fate of mercury species in highly polluted brownfields by means of thermal desorption. J. Hazard Mater. 325, 1–7. https://doi.org/10.1016/j.jhazmat.2016.11.068.
Saiz-Lopez, A., Sitkiewicz, S.P., Roca-Sanjuán, D., Oliva-Enrich, J.M., Dávalos, J.Z., Notario, R., Jiskra, M., Xu, Y., Wang, F., Thackray, C.P., Sunderland, E.M., Jacob, D. J., Travnikov, O., Cuevas, C.A., Acuña, A.U., Rivero, D., Plane, J.M.C., Kinnison, D. E., Sonke, J.E., 2018. Photoreduction of gaseous oxidized mercury changes global atmospheric mercury speciation, transport and deposition. Nat. Commun. 9, 4796. https://doi.org/10.1038/s41467-018-07075-3.
Salata, S., Peccol, E., Borsato, O., 2019. A Framework to evaluate land take control policy efficiency in friuli Venezia Giulia, Italy. Sustain. Times 11, 6406. https://doi.org/10.3390/su11226406.
Schlüter, K., 2000. Review: evaporation of mercury from soils. An integration and synthesis of current knowledge. Environ. Geol. 39, 249–271. https://doi.org/10.1007/s002540050005.
Schuster, E., 1991. The behavior of mercury in the soil with special emphasis on complexation and adsorption processes - a review of the literature. Water, Air, Soil Pollut. 56, 667–680. https://doi.org/10.1007/BF00342308.
Selin, H., Keane, S.E., Wang, S., Selin, N.E., Davis, K., Bally, D., 2018. Linking science and policy to support the implementation of the Minamata Convention on Mercury. Ambio 47, 198–215. https://doi.org/10.1007/s13280-017-1003-x.
Sherman, L.S., Blum, J.D., Douglas, T.A., Steffen, A., 2012. Frost flowers growing in the Arctic ocean-atmosphere-sea ice-snow interface: 2. Mercury exchange between the atmosphere, snow, and frost flowers. J. Geophys. Res. Atmos. 117, D00R10. https://doi.org/10.1029/2011JD016186.
Shi, T., Gong, Y., Ma, J., Wu, H., Yang, S., Ju, T., Qu, Y., Liu, L., 2020. Soil-air exchange of mercury from agricultural fields in Zhejiang, East China: seasonal variations, influence factors, and models of fluxes. Chemosphere 249, 126063. https://doi.org/10.1016/j.chemosphere.2020.126063.
Sholupov, S., Pogarev, S., Ryzhov, V., 2004. Zeeman atomic absorption spectrometer RA-915 + for direct determination of mercury in air and complex matrix samples, 85, 473–485. https://doi.org/10.1016/j.fuproc.2003.11.003.
Sigler, J.M., Lee, X., 2006. Gaseous mercury in background forest soil in the northeastern United States. J. Geophys. Res. Biogeosciences 111, G02007. https://doi.org/10.1029/2005JG000106.
Sigura, M., Boscutti, F., Buccheri, M., Dorigo, L., Glerean, P., Lapini, L., 2017. La REL dei paeasaggi di pianura, di area Montana e urbanizzati. Piano Paesaggistico regionale del Friuli-Venezia Giulia (Parte Strategica) E1-allegato alla scheda di RER. Reg. Friuli -Venezia Giulia 84. http://www.regione.fvg.it/rafvg/cms/RAFVG/ambiente-territorio/pianificazione-gestione-territorio/FOGLIA21/#id9.
Sizmur, T., McArthur, G., Risk, D., Tordon, R., O'Driscoll, N.J., 2017. Gaseous mercury flux from salt marshes is mediated by solar radiation and temperature. Atmos. Environ. 153, 117–125. https://doi.org/10.1016/j.atmosenv.2017.01.024.
Skyllberg, U., Drott, A., 2010. Competition between disordered iron sulfide and natural organic matter associated thiols for mercury(II) - an EXAFS study. Environ. Sci. Technol. 44, 1254–1259. https://doi.org/10.1021/es902091w.
Sommar, J., Osterwalder, S., Zhu, W., 2020. Recent advances in understanding and measurement of Hg in the environment: surface-atmosphere exchange of gaseous elemental mercury (Hg0). Sci. Total Environ. 721, 137648 https://doi.org/10.1016/j.scitotenv.2020.137648.
Sommar, J., Zhu, W., Shang, L., Lin, C.J., Feng, X., 2016. Seasonal variations in metallic mercury (Hg0) vapor exchange over biannual wheat-corn rotation cropland in the North China Plain. Biogeosciences 13, 2029–2049. https://doi.org/10.5194/bg-13-2029-2016.
Stamenkovic, J., Gustin, M.S., 2009. Nonstomatal versus stomatal uptake of atmospheric mercury. Environ. Sci. Technol. 43, 1367–1372. https://doi.org/10.1021/es801583a.
Stamenkovic, J., Gustin, M.S., Arnone, J.A., Johnson, D.W., Larsen, J.D., Verburg, P.S.J., 2008. Atmospheric mercury exchange with a tallgrass prairie ecosystem housed in mesocosms. Sci. Total Environ. 406, 227–238. https://doi.org/10.1016/j.scitotenv.2008.07.047.
Streets, D.G., Horowitz, H.M., Lu, Z., Levin, L., Thackray, C.P., Sunderland, E.M., 2019. Five hundred years of anthropogenic mercury: spatial and temporal release profiles. Environ. Res. Lett. 14, 084004 https://doi.org/10.1088/1748-9326/ab281f.
Sun, Y., Guo, Z., Du, J., Zhao, W., 2020a. Diffuse emission and transport of gaseous elemental mercury (GEM) in the Mapamyum geothermal system, Western Tibet (China). J. Volcanol. Geoth. Res. 397, 106825 https://doi.org/10.1016/j.jvolgeores.2020.106825.
Sun, S., Ma, M., He, X., Obrist, D., Zhang, Q., Yin, X., Sun, T., Huang, J., Guo, J., Kang, S., Qin, D., 2020b. Vegetation mediated mercury flux and atmospheric mercury in the alpine permafrost region of the central Tibetan plateau. Environ. Sci. Technol. 54, 6043–6052. https://doi.org/10.1021/acs.est.9b06636.
Sysalová, J., Kučera, J., Drtinová, B., Červenka, R., Zvěřina, O., Komárek, J., Kameník, J., 2017. Mercury species in formerly contaminated soils and released soil gases. Sci. Total Environ. 584 (585), 1032–1039. https://doi.org/10.1016/j.scitotenv.2017.01.157.
Tao, Z., Liu, Y., Zhou, M., Chai, X., 2017. Exchange pattern of gaseous elemental mercury in landfill: mercury deposition under vegetation coverage and interactive effects of multiple meteorological conditions. Environ. Sci. Pollut. Res. 24, 26586–26593. https://doi.org/10.1007/s11356-017-0275-9.
Tassi, F., Cabassi, J., Calabrese, S., Nisi, B., Venturi, S., Capecchiacci, F., Giannini, L., Vaselli, O., 2016. Diffuse soil gas emissions of gaseous elemental mercury (GEM)

from hydrothermal-volcanic systems: an innovative approach by using the static closed-chamber method. Appl. Geochem. 66, 234–241. https://doi.org/10.1016/j.apgeochem.2016.01.002.
Teršič, T., Gosar, M., Biester, H., 2011. Distribution and speciation of mercury in soil in the area of an ancient mercury ore roasting site, Frbejžene trate (Idrija area, Slovenia). J. Geochem. Explor. 110, 136–145. https://doi.org/10.1016/j.gexplo.2011.05.002.
Terzano, R., Santoro, A., Spagnuolo, M., Vekemans, B., Medici, L., Janssens, K., Göttlicher, J., Denecke, M.A., Mangold, S., Ruggiero, P., 2010. Solving mercury (Hg) speciation in soil samples by synchrotron X-ray microspectroscopic techniques. Environ. Pollut. 158, 2702–2709. https://doi.org/10.1016/j.envpol.2010.04.016.
Treu, F., Zini, L., Zavagno, E., Biolchi, S., Boccali, C., Gregorič, A., Napolitanoc, R., Urbancd, J., Zuecco, G., Cucchi, F., 2017. Intrinsic vulnerability of the Isonzo/Soča high plain aquifer (NE Italy - W Slovenia). J. Maps 13, 799–810. https://doi.org/10.1080/17445647.2017.1384935.
U.S. EPA, 1998. Method 7473 (SW-846): Mercury in Solids and Solutions by Thermal Decomposition, Amalgamation, and Atomic Absorption Spectrophotometry. Revision 0, Washington, DC.
USDA, 1987. USDA Textural Soil Classification. Soil Mech. Lev. I Modul. 3. USDA Textural Soil Classif.
Wallschläger, D., Turner, R.R., London, J., Ebinghaus, R., Kock, H.H., Sommar, J., Xiao, Z., 1999. Factors affecting the measurement of mercury emissions from soils with flux chambers. J. Geophys. Res. Atmos. 104, 21859–21871. https://doi.org/10.1029/1999JD900314.
Walters, N.E., Glassford, S.M., Van Heyst, B.J., 2016. Mercury flux from naturally enriched bare soils during simulated cold weather cycling. Atmos. Environ. 129, 134–141. https://doi.org/10.1016/j.atmosenv.2016.01.029.
Wang, D., He, L., Shi, X., Wei, S., Feng, X., 2006. Release flux of mercury from different environmental surfaces in Chongqing, China. Chemosphere 64, 1845–1854. https://doi.org/10.1016/j.chemosphere.2006.01.054.
Wang, S., Feng, X., Qiu, G., Wei, Z., Xiao, T., 2005. Mercury emission to atmosphere from Lanmuchang Hg-Tl mining area, Southwestern Guizhou, China. Atmos. Environ. 39, 7459–7473. https://doi.org/10.1016/j.atmosenv.2005.06.062.
Wickham, H., Chang, W., Henry, L., Pendersen, T.L., Takahashi, K., Wilke, C., Woo, K., Yutani, H., Dunnington, D., 2016. ggplot2: Elegant Graphics for Data Analysis. Springer-Verlag, New York.
Yan, J., Wang, C., Wang, Z., Yang, S., Li, P., 2019. Mercury concentration and speciation in mine wastes in Tongren mercury mining area, southwest China and environmental effects. Appl. Geochem. 106, 112–119. https://doi.org/10.1016/j.apgeochem.2019.05.008.
Yang, Y.K., Zhang, C., Shi, X.J., Lin, T., Wang, D.Y., 2007. Effect of organic matter and pH on mercury release from soils. J. Environ. Sci. 19, 1349–1354. https://doi.org/10.1016/S1001-0742(07)60220-4.
Yin, R., Feng, X., Wang, J., Li, P., Liu, J., Zhang, Y., Chen, J., Zheng, L., Hu, T., 2013. Mercury speciation and mercury isotope fractionation during ore roasting process and their implication to source identification of downstream sediment in the Wanshan mercury mining area, SW China. Chem. Geol. 336, 72–79. https://doi.org/10.1016/j.chemgeo.2012.04.030.
Yuan, W., Wang, X., Lin, C.J., Sommar, J., Lu, Z., Feng, X., 2019. Process factors driving dynamic exchange of elemental mercury vapor over soil in broadleaf forest ecosystems. Atmos. Environ. 219, 117047 https://doi.org/10.1016/j.atmosenv.2019.117047.
Zhang, G., Zhou, X., Li, Xu, Wang, L., Li, Xiangyun, Luo, Z., Zhang, Y., Yang, Z., Hu, R., Tang, Z., Wang, D., Wang, Z., 2021. Gaseous elemental mercury exchange fluxes over air-soil interfaces in the degraded grasslands of northeastern China. Biology 10, 917. https://doi.org/10.3390/biology10090917.
Zhang, T., Kim, B., Levard, C., Reinsch, B.C., Lowry, G.V., Deshusses, M.A., Hsu-Kim, H., 2012. Methylation of mercury by bacteria exposed to dissolved, nanoparticulate, and microparticulate mercuric sulfides. Environ. Sci. Technol. 46, 6950–6958. https://doi.org/10.1021/es203181m.
Zhao, M., Running, S.W., 2010. Drought-induced reduction in global terrestrial net primary production from 2000 through 2009. Science 329, 940–943. https://doi.org/10.1126/science.1192666.
Zhou, J., Wang, Z., Zhang, X., Driscoll, C.T., 2021. Measurement of the vertical distribution of gaseous elemental mercury concentration in soil pore air of subtropical and temperate forests. Environ. Sci. Technol. 55, 2132–2142. https://doi.org/10.1021/acs.est.0c05204.
Zhou, J., Wang, Z., Zhang, X., Sun, T., 2017. Investigation of factors affecting mercury emission from subtropical forest soil: a field controlled study in southwestern China. J. Geochem. Explor. 176, 128–135. https://doi.org/10.1016/j.gexplo.2015.10.007.
Zhu, J., Wang, D., Liu, X., Zhang, Y., 2011. Mercury fluxes from air/surface interfaces in paddy field and dry land. Appl. Geochem. 26, 249–255. https://doi.org/10.1016/j.apgeochem.2010.11.025.
Zhu, W., Li, Z., Li, P., Yu, B., Lin, C.J., Sommar, J., Feng, X., 2018. Re-emission of legacy mercury from soil adjacent to closed point sources of Hg emission. Environ. Pollut. 242, 718–727. https://doi.org/10.1016/j.envpol.2018.07.002.
Žibret, G., Gosar, M., 2006. Calculation of the mercury accumulation in the Idrijca River alluvial plain sediments. Sci. Total Environ. 368, 291–297. https://doi.org/10.1016/j.scitotenv.2005.09.086.